



## EDITORIAL BOARD

### Editor-in-Chief

J. A. Hudson

*Imperial College of Science, Technology & Medicine, London, UK*

### Senior Editors

E. T. Brown  
University of Queensland  
Brisbane, Australia

C. Fairhurst  
University of Minnesota  
Minneapolis, MN, USA

E. Hoek  
University of Toronto  
Canada

# COMPREHENSIVE ROCK ENGINEERING

*Principles, Practice & Projects*

### Editor-in-Chief

JOHN A. HUDSON

*Imperial College of Science, Technology & Medicine, London, UK*

## INTERNATIONAL ADVISORY BOARD

G. Barla

*Politecnico di Torino, Italy*

J.-C. Roegiers

*University of Oklahoma, Norman, OK, USA*

Y. D. Diadkin

*St. Petersburg Mining Institute, Russia*

M. Romana

*Universidad Politecnica de Valencia, Spain*

P. Londe

*Pierre Londe & Associates, Puteaux, France*

O. Stephansson

*Royal Institute of Technology  
Stockholm, Sweden*

Y. Nishimatsu

*University of Tokyo, Japan*

Tan Tjong Kie

*Chinese Academy of Sciences, Beijing, China*

Y. Ohnishi

*University of Kyoto, Japan*

H. Wagner

*Chamber of Mines, Johannesburg, South Africa*

T. Ramamurthy

*Indian Institute of Technology, New Delhi, India*

W. A. Wittke

*Technische Hochschule Aachen, Germany*

### Volume 1

## FUNDAMENTALS

### Volume Editor

EDWIN T. BROWN

*University of Queensland, Brisbane, Australia*

LIBRARY, CSIRO  
WA LABORATORIES  
PRIVATE BAG NO 5  
WEMBLEY WA 6913



**PERGAMON PRESS**  
**OXFORD · NEW YORK · SEOUL · TOKYO**

## 2

# The Significance of Structural Geology in Rock Mechanics

BRUCE E. HOBBS

*CSIRO, Mount Waverley, Victoria, Australia*

---

2.1	INTRODUCTION	25
2.2	STRUCTURES IN ROCK MASSES	27
2.2.1	<i>General Statement</i>	27
2.2.2	<i>Nonpenetrative Structures</i>	28
2.2.2.1	<i>Fracture sets and systems</i>	28
2.2.2.2	<i>Fracture surfaces</i>	29
2.2.2.3	<i>Relations of fractures to other structures</i>	30
2.2.2.4	<i>Origin of fractures</i>	30
2.2.3	<i>Penetrative Structures</i>	32
2.2.3.1	<i>General statement</i>	32
2.2.3.2	<i>Linear structures (lineations)</i>	33
2.2.3.3	<i>Planar structures (foliations)</i>	33
2.3	FRACTAL GEOMETRY AND NONLINEAR DYNAMICS	35
2.3.1	<i>General Statement</i>	35
2.3.2	<i>Nonlinear Dynamics and Fractal Geometries</i>	38
2.3.3	<i>Fractals and Fractal Dimension</i>	41
2.3.4	<i>Affine Transformations and Iterated Function Systems (IFS)</i>	43
2.3.5	<i>Fractal Interpolation Functions</i>	46
2.4	FRACTAL REPRESENTATION OF THE PROFILES OF SINGLE JOINTS AND OF JOINT ROUGHNESS	49
2.4.1	<i>Fractal Representation of Profiles</i>	49
2.4.2	<i>Joint Roughness</i>	49
2.5	JOINT SYSTEMS	51
2.5.1	<i>Simple Joint Sets</i>	51
2.5.1.1	<i>The statistical approach to discontinuity geometry</i>	51
2.5.1.2	<i>Joint sets</i>	51
2.5.2	<i>Complicated Joint Systems</i>	54
2.6	FOLD SYSTEMS	56
2.7	CONCLUDING REMARKS	57
2.8	REFERENCES	60

---

## 2.1 INTRODUCTION

The stability of excavations and the mechanical response of a rock mass during an excavation sequence are both commonly critically dependent upon the structure of the rock mass. Increasingly, as ore bodies and large civil engineering projects are developed within the tectonically active environments of the circum-Pacific region or within the structurally disturbed PreCambrian terrains of the Earth's crust, it becomes important to understand the detailed structural geology and deformation history of rock masses before excavation design begins.

It is fundamental that in structurally complicated terrains simple empirical collection of structural data is insufficient to gain a detailed understanding of the structure of a rock mass and therefore to enable meaningful design to take place. It is paramount that a detailed structural analysis be undertaken, as discussed in text books such as Turner and Weiss [1], Ramsay [2, 3], Hobbs *et al.* [4], and Price and Cosgrove [5]. This chapter is concerned with an introduction to the complexities commonly observed in structurally disturbed terrains and, in particular, focuses on geometric complexity and the ways in which such complexity may be understood and described using modern concepts arising from the dynamics of nonlinear systems.

The stability and mechanical response of a rock mass depend upon its mechanical properties and constitutive behavior, and upon the loading sequence imposed during excavation. We are not concerned with the loading sequence here, only the features of the rock mass which influence the mechanical properties and the constitutive behavior.

The mechanical properties and the constitutive behavior of rock masses depend upon: (i) the physical and chemical conditions of deformation; (ii) the mineralogical make-up of the rock; and (iii) the structure of the rock mass, in particular, the ways in which discontinuities or surfaces and lines of weakness are distributed and oriented with respect to the loads imposed by excavation or construction.

Most rocks that are encountered in engineering investigations are crossed by a number of such discontinuities of one sort or another that are potential planes or lines of failure associated with any future construction or excavation. By far the majority of these discontinuities were introduced during deformation in past geological times.

The mechanical properties and the behavior of rock masses are strongly influenced by not only the orientations of discontinuities with respect to imposed loads but by the spatial distribution of these discontinuities within the rock mass. Such orientations and spatial distributions are far from regular (see Figures 1 and 2) and considerable effort has been exerted over the years in describing such distributions from a statistical point of view. For the most part, these statistical distributions are empirical in nature and serve little predictive value. It is one of the aims of this chapter to point out that the geometry of these orientations and spatial distributions is fractal in form and that there are strong reasons in the mechanics of formation of these structures why such fractal geometries should develop.

Recognition of the fractal nature of the geometry of discontinuities in rock masses leads to a deeper understanding of their apparently irregular geometry and to the possibility of defining the probability of occurrence of structures within volumes of rock of engineering interest.

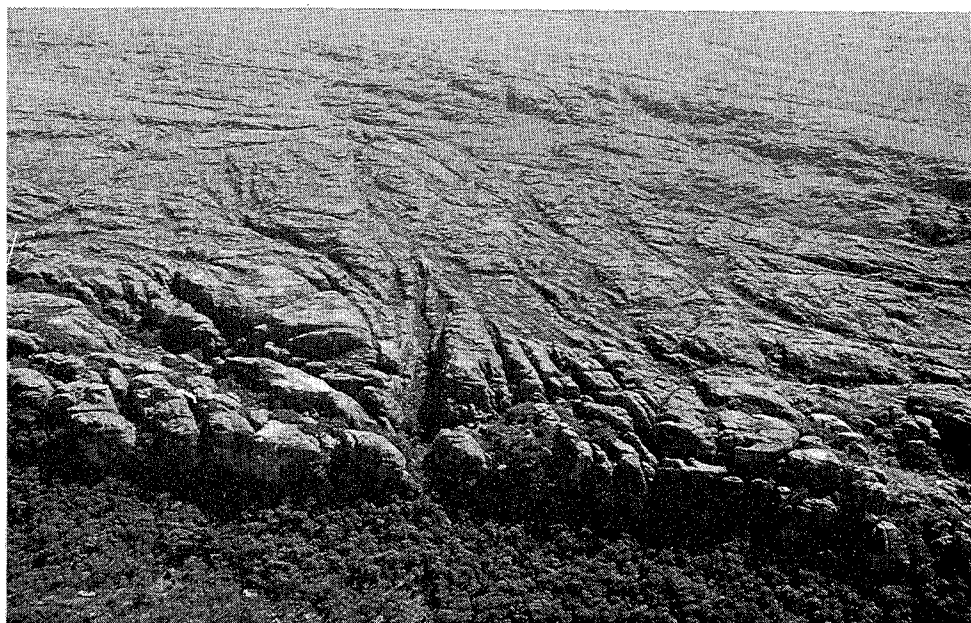
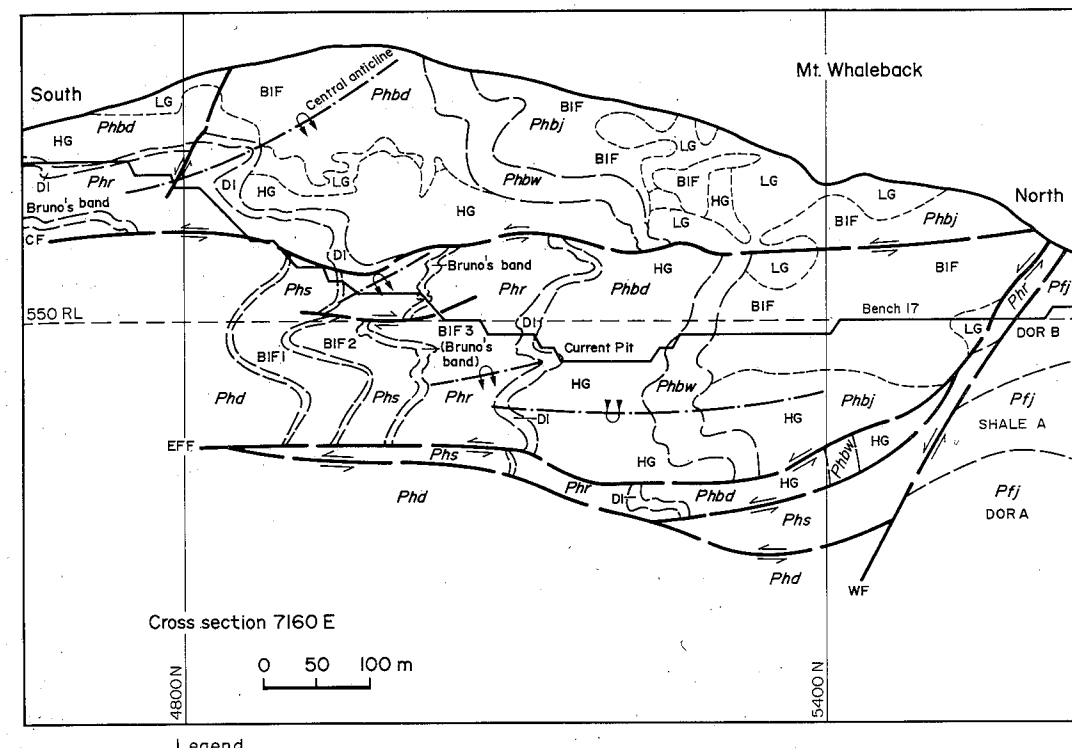


Figure 1 Joint system in the Kombolgie Sandstone. Looking East in the Southern Alligator River area, Northern Territory, Australia



Legend

<i>Phbj</i>	Joffre member	<i>High angle normal fault</i>
<i>Phbw</i>	Whaleback shale member	<i>Low angle normal fault</i>
<i>Phbd</i>	Dales gorge member	<i>Whaleback fault</i>
<i>Phr</i>	Mt. McRae shale	<i>Central fault</i>
<i>Phs</i>	Mt. Sylvia formation	<i>Overturned syncline</i>
<i>Phd</i>	Wittenoom dolomite	<i>Overturned anticline</i>
<i>Pfj</i>	Jeerinah formation	<i>High grade ore</i>
<i>DOR B</i>	Dolerite B	<i>Low grade ore</i>
<i>SHALE A</i>	SHALE A	<i>Banded iron formation</i>
<i>DOR A</i>	Dolerite A	<i>Fault showing relative displacement</i>
<i>Fbu</i>	Upper mafic volcanic unit of Fortescue group	

Figure 2 North-South section across the Mt. Whaleback open pit iron ore mine, Newman, Western Australia. Published with permission of Janos Ronaszek

The plan of this chapter is as follows: in Section 2.2 we look briefly at the common structures that exist within rock masses; in Section 2.3 we review those aspects of fractal geometry that are of importance for structural geology and briefly examine the broad mechanical principles that govern the development of such structures, and that imply that a fractal geometry may be the expected geometry for these structures; in Section 2.4 we examine the structure of single discontinuity surfaces and discuss whether there is a correlation between the fractal dimension of these surfaces and the Joint Roughness Coefficient (JRC) [6]; in Section 2.5 we examine the geometry of single joints and joint sets and progress to examine the geometry of complicated joint systems; in Section 2.6, we briefly investigate the fractal geometry of folded surfaces and finally in Section 2.7, draw some conclusions regarding the importance of a fractal description of rock structural geometry for engineering purposes.

## 2.2 STRUCTURES IN ROCK MASSES

### 2.2.1 General Statement

Any portion of the Earth will generally be acted upon by forces which tend to displace and to distort the rocks within that region. Some of these forces arise solely from the weight of the overlying

rocks; others arise from large-scale motions of material composing adjacent parts of the crust or of the mantle of the Earth. In some instances, these forces are small or act only for short periods of time so that no significant deformation results. In other instances, the forces act for relatively long periods of time and spectacular permanent deformations, such as large-scale folding, result. In still other instances, the fracture strength of the rocks may be exceeded and faulting and jointing are then the most conspicuous modes of deformation. Whether the rocks composing a region deform permanently or not and whether any deformation is predominantly by folding, by faulting, by jointing or by yet other modes, depends upon the interplay of a large number of physical and chemical factors including the temperature, the hydrostatic pressure, the pressure of any pore fluids, the rate at which the deforming forces are applied, the rate at which deformation proceeds and the composition (including the fluid chemical composition) of the rocks. On the whole then, we can expect the rocks that we meet in engineering investigations to have been deformed in one or more of a number of different ways, thus introducing a large array of different kinds of discontinuities.

Broadly speaking, it is useful to distinguish two types of structures in rock masses referred to by structural geologists as penetrative structures and nonpenetrative structures.

A particular structure is said to be penetrative within a rock mass if, on the scale under consideration, that structure is repeated over and over again, with much the same spacing and orientation pattern from one sample of the rock mass to the next. Otherwise, the structure is nonpenetrative, that is, the structure may occur within different samples from a rock mass, but its distribution, spacing and orientation are not similar from one sample to the next.

Typical of penetrative structures that influence mechanical properties and behavior are the flow foliations of igneous rocks, the bedding surfaces of sedimentary rocks and the lineations and foliations of regionally deformed metamorphic rocks.

Typical of the nonpenetrative structures of interest here are the joint surfaces and faults characteristic of all types of rocks. These are the structures most commonly considered by engineering geologists mainly because they are the most obvious discontinuities in many rock masses. However, penetrative structures such as slaty cleavage and schistosity can at times be much more important in controlling mechanical behavior even though they are not features that need be visually prominent in drill cores or fresh exposures.

In what follows, these two classes of structure are considered separately, particular attention being paid to purely descriptive characteristics. Nonpenetrative structures are considered first.

## 2.2.2 Nonpenetrative Structures

The most common nonpenetrative structures encountered in rock masses are joints and faults. Both are different types of fractures and have suffered different displacement histories.

Thus, joints and faults are structures resulting from brittle behavior, in which blocks of rock are displaced relative to one another across narrow and approximately planar discontinuities. The discontinuities are called joints if the component of displacement parallel to the structure is zero (or too small to be apparent to the unaided eye) or faults if the surface parallel component of displacement is larger.

### 2.2.2.1 Fracture sets and systems

Fractures usually occur as families with more or less regular spacing in a given rock type. We define a fracture set as a group of fractures of common origin. The fractures of a set are often approximately parallel to one another, but they need not be. For example, a group of fractures that are everywhere parallel to a fold hinge line and perpendicular to bedding may comprise a genetically distinct set even though the fractures are not all parallel to one another. Fractures of several sets commonly occur together, giving exposures a blocky or fragmented appearance (see Figure 3).

The whole assemblage of fractures present in an exposure or map area is called a fracture system (see Figure 1). Typically the characteristics of a fracture system, that is the sizes, spacings and orientations of the fractures, are seen to vary in some degree across contacts between rocks of different lithology. This fact is put to use in mapping contacts, particularly in air-photo interpretation or in surface mapping of heavily weathered or inaccessible exposures. In a given area, there may also be revealing differences in the fracture systems at limb and hinge positions on large folds, or at different distances from large faults.



Figure 3 Joint systems in Heavitree Quartzite, Ormiston Gorge, Northern Territory, Australia

### 2.2.2.2 Fracture surfaces

The conspicuous fracture surfaces in most outcrops have dimensions ranging from tens of centimeters to hundreds of meters and are repeated at distances of several centimeters to tens of meters. In addition, most rocks contain numerous inconspicuous fractures of smaller size and close spacing, many of them visible only in thin section. Fractures small enough to require microscopic observation are called microjoints [7] or microfractures [8]. Any fractures that are larger than associated fractures of the same orientation are called master fractures. The master fractures seen in aerial photographs can sometimes be traced for distances of many kilometers.

Fractures in massive rocks, like some sandstones, may show distinctive patterns of surface relief [5, 9–14]. The most common type is called plume structure. Markings similar to plume structure are seen on fracture surfaces in glass and other brittle materials [15] and can be interpreted in terms of the direction of propagation of the fracture front.

Some fractures are barren hair-line cracks or empty fissures, but many contain coatings or narrow veins of secondary minerals, very commonly quartz or calcite. These deposits along fracture planes can be classified as dilational if the vein material occupies space between the two original fracture surfaces, or as nondilational if the vein material occupies space outside the two original fracture surfaces, that is the vein has developed by replacement of the original rock. Several criteria for distinguishing dilational from nondilational veins are illustrated in Figure 4, and others are discussed by Park and McDiarmid [16]. Notice that it is entirely possible to have replacement together with dilation of a fracture, so that some kinds of evidence for replacement (e.g. Figure 4) are not necessarily evidence against dilation.

It is important in any study of fractures to examine thin sections across the fracture for details of mineralogy, microstructure and displacements because such observations are essential for working out the relative ages of several fracture sets and for relating fracture history to events in the thermal and mechanical history. In engineering practice, the mineralogy and texture of fracture fillings is important because fractures with different fillings can have different mechanical properties and different properties governing storage and flow of fluids.

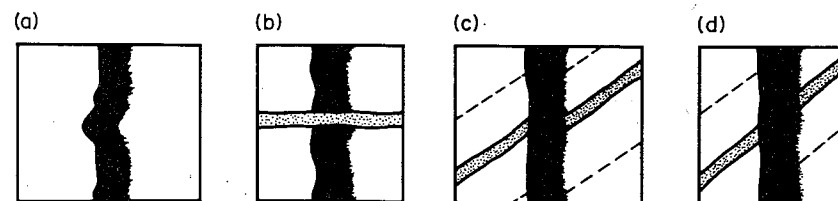


Figure 4 Criteria for distinguishing dilational (D) and nondilational (N) fractures. (a) Opposite sides match – D, (b) resistant vein crosses – N, (c) offset of markers – D, (d) no offset of markers – N

### 2.2.2.3 Relations of fractures to other structures

In layered rocks of all kinds the most prominent fractures usually intersect the layering at high angles. Where the layers are folded, fractures in various special orientations relative to the folds are seen. These fractures are described with respect to orthogonal reference axes,  $a$ ,  $b$ ,  $c$ ; where  $b$  is parallel to the fold hinge line,  $a$  is normal to the hinge line and lies in the axial plane, and  $c$  is normal to the  $a$ - $b$  plane (Figure 5). Fractures approximately perpendicular to fold axes are thus called  $a$ - $c$  fractures. Fractures parallel to fold axes and approximately perpendicular to layering are called radial fractures. Fractures in paired sets of the type represented by 4 in Figure 5 can be called  $(0kl)$  fractures. It is emphasized that the reference axes  $a$ ,  $b$  and  $c$ , while useful for describing fracture orientations, have no simple significance in terms of the displacement or strain fields represented by the fractures or folds. The belief, widely held 30–40 years ago, that the  $a$  direction was necessarily a special direction of ‘movement’ or of ‘tectonic transport’ has been discarded. Excellent examples of fractures associated with folds are described by Norris [17], Sterns [18] and Handin *et al.* [19].

Fractures associated with faults may predate the faults and have no genetic relation to the faults apart from a possible control on the orientation of the fault planes. Other fractures may be intimately related to faulting and useful in revealing the sense of slip on faults. The best known examples here are the feather joints of Cloos [20] or other pinnate fractures. These occur preferentially in the immediate vicinity of a fault plane and intersect the fault in an acute angle pointing in the direction of relative movement of the block containing the pinnate fractures. Pinnate fractures can evidently form both in advance of the development of a through-going fault plane or during subsequent slip on a fault. They have been observed in experiments on a wide variety of rocks and other materials [21–25].

Fracture systems in igneous rock bodies may be quite different from fracture systems in the surrounding rock and they are often symmetrically related to the contacts of the body, suggesting an origin during emplacement and cooling. One prominent fracture set is commonly seen at a high angle to the nearest contact. Balk [26] and Price [13] give detailed descriptions of these and other fractures in plutonic bodies. In tabular bodies such as flows, dikes or sills, fractures perpendicular to the contacts are again common and may display a special configuration known as columnar jointing, in which the fractures isolate elongate prisms with more or less regular hexagonal cross sections. The field worker in an area of poor exposure may be able to use well developed columnar jointing as an indicator of the normal to the contacts of a tabular body. This interpretation is not always reliable, however because curved columnar jointing oblique to contacts is also well known [27].

### 2.2.2.4 Origin of fractures

#### (i) Extension and shear fractures

A genetic classification of fractures is based on the size of the shear component of displacement at the moment of origin. If a fracture forms with a shear component that is zero, so that the total displacement is directed normal to the fracture surfaces, the structure is an extension joint (Figure 6a). If the shear component has some finite value, the structure is a shear joint (Figure 6b).

Thus, a shear joint is in fact a fault but commonly the displacement is so small that it is difficult to detect without thin section examination. However, from an engineering viewpoint it is important to make the distinction between extension joints and shear joints because the two different classes of fractures are commonly associated with completely different types of surface markings and coatings resulting in contrasting mechanical properties.

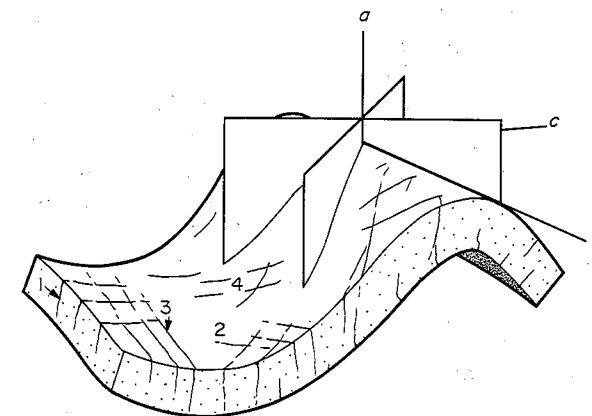


Figure 5 Joint sets associated with folding: 1:  $ac$  joints, 2: paired sets normal to bedding and symmetrical about  $ac$ , 3: radial or  $(h0l)$  joints, 4:  $(0kl)$  joints intersecting in a

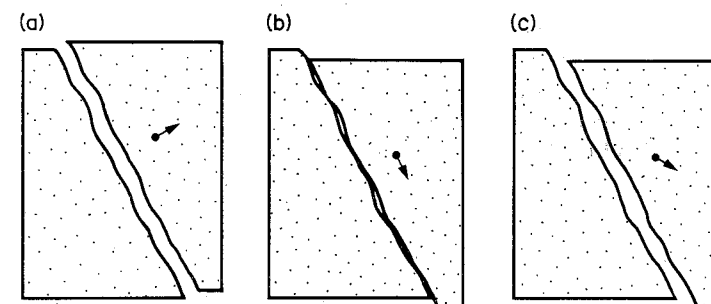


Figure 6 (a) Extensional joints, (b) shear joints, (c) extensional joints with shear

In what follows the term joint is used in place of fracture where one is not too interested in the displacement history. The terms extension joint and shear joint are used to qualify the displacement history and the term fault is used for any shear joint for which the displacement is considered large on the scale under consideration.

Following the initial displacement at the inception of a joint, there may be a long and complex history of further displacements. This is indicated by joints carrying successive secondary mineral coatings in each of which there are differently oriented slickenside striae or fibrous mineral growths [28].

Extension joints in isotropic rocks form normal to one of the principal directions of stress, otherwise there would exist a finite shearing stress on the potential joint plane at the moment before fracture and a corresponding finite shear displacement would occur. In the usual laboratory tests and presumably in most natural environments, extension joints form normal to the direction of  $\sigma_3$  ( $\sigma_1$ ,  $\sigma_2$ ,  $\sigma_3$  are the axes of maximum, intermediate and minimum principal compressive stress at any point in the rock mass) [29]. Shear joints can form at any angle to the principal directions of stress other than  $90^\circ$ .

Various criteria have been suggested to allow distinction between extension joints and shear joints. These include surface markings, regional orientation patterns, and relations to other structures. Thus, a joint set lacking slickensides and oriented normal to the hinge line of a doubly plunging anticline might be interpreted as a set of extension joints. While a convincing case can sometimes be built up from many lines of evidence, it is usually impossible to determine whether a joint set originated as extension or shear joints although some details of subsequent displacements may be determined. The terms extension joint and shear joint are not suitable field terms because thin section observations, commonly, are required to determine the nature of the displacements.

(ii) *Joints due to erosional unloading in isotropic rocks*

Some joints form during erosional unloading, on account of the greater ease with which decompressed rock expands normal to, rather than parallel to, the free surface. Imagine that a rock mass consists of isotropic rock at depth, in which all shearing stresses have been relaxed by creep processes. The body will only remain in a state of hydrostatic stress during erosional unloading if extension is equal in all directions. Near the surface upward extension may commonly be easier than horizontal extension because the normal stress on horizontal planes must approach that due to atmospheric pressure, whereas this is not necessarily true for the normal stress on vertical planes. The state of stress may therefore become nonhydrostatic with  $\sigma_3$  approximately perpendicular to the Earth's surface. Extension joints formed in this situation would be about parallel to the surface of the Earth, and this is an explanation for the sets of flat-lying joints in granitic rocks referred to as sheeting or sheet structure [30, 31]. The amount of expansion to be expected from stress relief during erosion is indicated by the values for the compressibility of the rock. For near-surface conditions, typical compressibilities fall in the range  $10^{-4}$  MPa to  $10^{-5}$  MPa [32]. Pressure changes to 200 MPa, corresponding with depth changes of about 6 km lead to volume changes ranging from a few percent to a few tenths of a percent. If such volume changes are accomplished mainly by vertical extension, and if this extension takes place fast enough, horizontal extension joints may form.

(iii) *Joints due to differential volume changes in heterogeneous bodies*

Most big rock bodies and many small ones consist of several rock types juxtaposed in layers or other configurations. When such bodies are decompressed or cooled from conditions of hydrostatic stress, local deviatoric stresses will be set up within them because of the differences in compressibilities or thermal expansion coefficients between adjacent units of different lithology. Local deviatoric stresses will also be set up on a granular scale, where adjacent mineral grains of different orientations or composition will tend to undergo slightly different strains during decompression or cooling. Local nonhydrostatic stresses generated by decompression or cooling may be important in joint formation even where the original state of stresses is itself nonhydrostatic or where the total state of stress is governed by regional deformation as well as by the internal make-up of a rock body.

One clear example of jointing brought about by differential volume change is provided by the columnar jointing in sills [33, 34]. Imagine that a layer comprises a sill of hot igneous rock that is contracting more than the cooler layers of country rock on either side. Vertical contraction of the sill is accommodated by downward movement of the overlying country rock. But horizontal contraction of the sill is resisted by the country rock, assuming the sill contracts more in a given interval of time than the country rock. If the boundary between the two rock types is to remain coherent, then compressional structures must develop in the country rock or extensional structures must develop in the sill. If the sill is weaker in extension than the country rock is in compression, vertical extension joints may develop in the sill. Good columnar arrangement of these joints is enhanced if the sill contracts equally in all horizontal directions and if thermal and mechanical properties are identical in all horizontal directions in the country rock.

(iv) *Joints due to regional deformation*

Many joints, and particularly those that cut through rocks of different lithologies, appear to be related directly to folds produced by regional deformation (see Figure 5). The folds may be pronounced features or barely perceptible regional upwarps or downwarps. Indeed a conceivable cause of regional jointing is the very gentle flexing of lithospheric plates to be expected when a plate changes latitude and thereby its radius of curvature [35, 36].

## 2.2.3 Penetrative Structures

### 2.2.3.1 General statement

Penetrative structures of interest in engineering applications are primary layering structures, such as bedding in sedimentary rocks and flow layering in igneous rocks, and secondary structures due to deformation such as lineation and foliation in regionally metamorphosed rocks.

On the scale of a single hand specimen or large exposure, penetrative structures pervade the rock mass more or less uniformly and do not appear as obvious discontinuities. For this reason they

might be erroneously taken as just part of the bulk properties of the rock and not recognized as the potential failure planes and lines that they undoubtedly are in many (especially metamorphic) rock masses.

Indeed, many engineering geologists have a preoccupation with joint surfaces as potential failure planes, to the exclusion of all other structures. Whilst such a preoccupation with fracture systems is probably safe enough in weakly deformed sedimentary and igneous rocks, it can potentially lead to disaster if a keen appreciation of the penetrative structures in metamorphic rocks is not also actively maintained.

Penetrative structures are commonly, but not invariably associated with a preferred orientation of minerals. This preferred orientation pervades the rock even on the scale of a thin section and so contributes an important mechanical anisotropy to a rock mass. The preferred orientation may be due to the alignment of inequant grains such as micas during sedimentation, compaction or deformation or may be due to alignment of crystallographic axes during cooling or deformation. Such crystallographic preferred orientations may have no obvious expression in hand specimens and only become apparent after optical or X-ray examination. The preferred alignment of microfractures might also exist in some rocks.

Preferred orientations of minerals and grains impart a mechanical anisotropy to the rock that might be expressed as an anisotropy of elastic properties, and so be important in any computational modeling of a rock mass. Alternatively it might be expressed as a directional difference in blasting properties or as a strong departure of fracture orientation from that to be expected in isotropic rock.

### 2.2.3.2 Linear structures (lineations)

The word lineation is used to describe any linear structure that occurs repetitively in a sample of rock; for example, it may refer to an array of elongate pebbles, oriented with their long dimensions mutually parallel, or it may refer to the lines of intersection of two foliations. It should not be confused with the word lineament which is used to describe linear topographic features of regional extent, that are believed to reflect crustal structure [37, 38]. Lineation may be a primary igneous [39] or sedimentary structure [40] but the most common are secondary structures related to deformation. Here we are concerned only with the latter.

Lineations are ubiquitous in deformed rocks and it is common for more than one lineation set to be visible on a given foliation plane (Figure 7). If related to a given group of folds they are generally, but not invariably, either parallel to the fold axis or inclined to the fold axis at a high angle. Many lineations are associated with a foliation and actually lie in that surface, but this is not necessarily so, and lineated rocks that are not foliated are fairly common, particularly in areas of gneissic rocks. It is commonplace for a single deformation to give rise to lineations of more than one orientation. Thus, for example, in slates, a lineation forms more or less parallel to the fold axes, whilst another forms in the cleavage plane at a high angle to the first.

Some examples of lineations are the axes of small-scale folds, the interactions of two sets of foliations, elongate mineral aggregates, the alignment of the long axes of minerals and pebbles, and rodding, mullion and boudinage structures [5].

Lineations are important mechanically in some rocks because the rock tends to fail as large pencil shaped blocks parallel to the lineation. At Broken Hill, NSW, for instance, many of the schists within the retrograde schist zones [41] are strongly lineated, almost to the exclusion of any foliation. This lineation is commonly steeply oriented. In underground openings, the roof commonly fails as blocks approximately equant in cross section but very long vertically parallel to the lineation. The lineation in fact defines a very strong anisotropy that, to the casual eye, is not obvious in drill core, but which controls the behavior in underground openings.

### 2.2.3.3 Planar structures (foliations)

Most rocks have planar discontinuities within them that are known variously under one or other of the names, bedding, cleavage or foliation. Bedding is a term applied mainly to sedimentary rocks and refers to the planar structure that develops during deposition from wind, water or ice. Bedding is defined by variations in grain size or mineralogical composition and is commonly the most obvious structure displayed in outcrop or drill core. Bedding surfaces, along with fracture systems are commonly the planes that control failure in sedimentary rocks and in excavations, or during blasting the rock mass normally breaks into parallelepipeds bounded by the bedding and two fracture sets

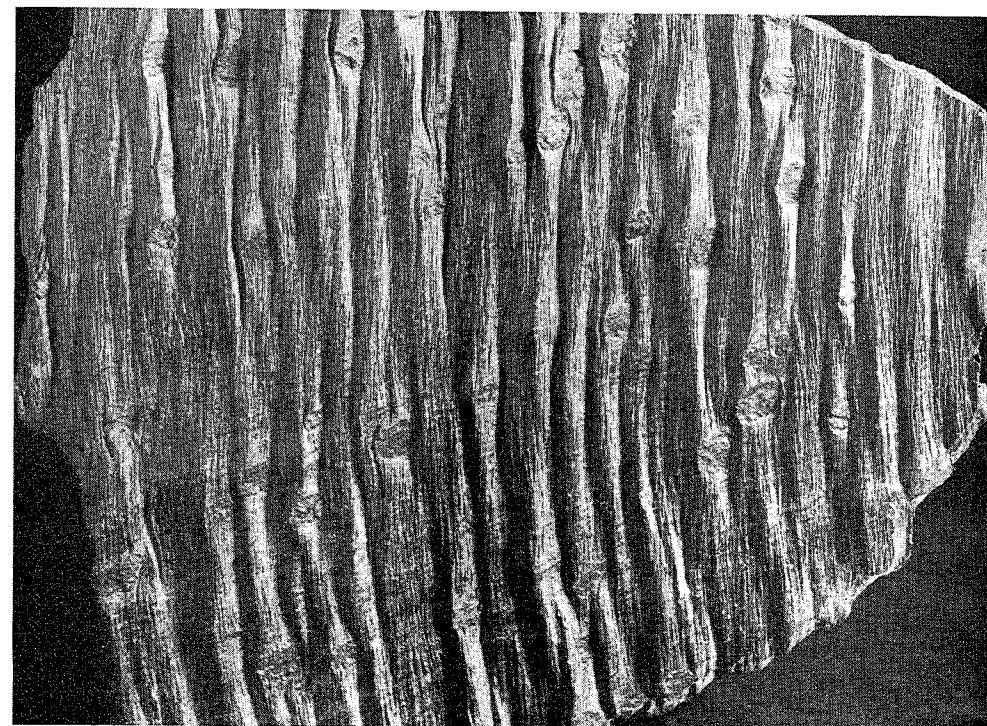


**Figure 7** Lineated foliation surface from White's open pit uranium mine, Rum Jungle, Northern Territory, Australia. The prominent lineation is composed of small crenulations. The less pronounced lineation trending upwards to the right is a bedding/foliation intersection. Small spots are altered porphyroblasts

approximately normal to the bedding. Parallel to the bedding there may be a preferred orientation of platy minerals such as mica or clay minerals and at times there may also be a preferred orientation of ellipsoidal sand grains. In some instances such a preferred orientation may be oblique to the bedding forming what is called an imbricate structure where ellipsoidal sand grains are stacked one against the other, inclined to the bedding but pointing in what was the downstream direction at the time of deposition. Such preferred orientations may produce a strong anisotropy in a rock mass that can at times control roof failure in coal mines.

In igneous rocks, particularly silica rich rocks that tend to be fairly viscous, a flow structure commonly develops as the molten rock is crystallizing. This structure is referred to as a flow foliation and may be defined by the preferred orientation of inequant crystals or xenoliths, or by segregation of different minerals into layers parallel to the flow planes. Flow foliation tends to be parallel to the contacts of igneous intrusions and fractures tend to be normal to the foliation so that, again, igneous rocks may tend to break into parallelepipeds bounded by the flow foliation and two fracture sets.

In metamorphic rocks there are commonly pervasive surfaces defined by discontinuities, preferred orientation of inequant minerals, laminar mineral aggregates or some combination of these microstructures (see Figure 8). In many cases these surfaces are inclined to bedding and since they have no counterpart in undeformed sedimentary rocks they must be the product of deformation. Elsewhere, however, bedding cannot be identified with certainty and it is not obvious whether the surface, or the earliest surface if there is more than one, is of sedimentary or of metamorphic origin; or in some instances it may even be a sedimentary surface that has been modified by metamorphism. For this reason there is a need for a nongenetic, general term to cover all surfaces found in deformed metamorphic rocks; we use the word foliation in this sense. Some geologists use the word foliation in a more restricted sense to refer only to surfaces produced by deformation and metamorphism. We do not subscribe to the latter usage because in many areas of deformed rocks it is difficult to decide just which surfaces are a product of deformation or of accompanying metamorphism. The term s-surface is used by some writers with the same meaning as foliation is used here.

In many areas of folded rocks there is a foliation inclined to the folded surface and systematically oriented with respect to the folds. These surfaces are generally approximately parallel to the axial planes of the folds in the hinge area and are therefore referred to as axial plane foliations.



**Figure 8** Thin section of crenulation cleavage from Cooma, NSW, Australia. View is 2 mm across

In fine grained rocks, such as slates, where the grain size of mica is too small to be resolved by eye, this structure is referred to as slaty cleavage and is the structure along which the rock will split with greatest ease. In coarser grained rocks such a structure is called a schistosity; if a mineral segregation is developed also in rocks rich in quartz and feldspar as well as micas, it might be called a gneissosity. All of these terms are more conveniently covered by the single term foliation unless the situation arises where one wants to be a little more specific.

It is important to emphasize that foliation in metamorphic rocks may not be visually obvious in fresh drill core or rock exposures. Under such circumstances, bedding and various types of fractures may be quite striking and are the structures commonly described and recorded. However, the foliation in metamorphic rocks may be the structure that controls completely what happens during blasting, roof bolting or other excavation practices. It is most commonly inclined to bedding and fracture sets, the inclination of the foliation being a function of where the locality is relative to large-scale fold hinges [5].

## 2.3 FRACTAL GEOMETRY AND NONLINEAR DYNAMICS

### 2.3.1 General Statement

Many geometrical aspects of joints, faults, shear zones and foliation surfaces have been described from a statistical point of view [42–46]. Such aspects include surface roughness, discontinuity spacing, discontinuity persistence, discontinuity orientation distributions, joint apertures and joint permeabilities. Attempts to describe these attributes in terms of statistical parameters recognize an intrinsic characteristic of discontinuities in rock masses, namely, that they are not perfectly regular in their orientations, shapes and sizes, but instead are somewhat irregular perhaps in a statistically definable manner. Such an observation is rationalized by statements such as 'Nature is never perfect' or 'irregularities are to be expected in Nature'.

Added to this observation that discontinuity attributes are never definable in terms of perfect geometrical parameters is the observation that discontinuities are repeated at all scales in a rock

mass. Thus, Figure 9 shows joints in a quartzite with the same patterns of distribution repeated at outcrops varying in size from  $10^8 \text{ m}^2$  down to  $1 \text{ m}^2$ ! This duplication of identical patterns of discontinuity orientation, spacing and spatial grouping over 8 orders of magnitude is astounding yet is an observation that is taken for granted by most structural geologists not only with respect to discontinuities but with respect to all structural features in deformed rocks. Thus it is mandatory to include a pocket knife, hand lens or coin as the scale in any photograph of a deformed rock; if such

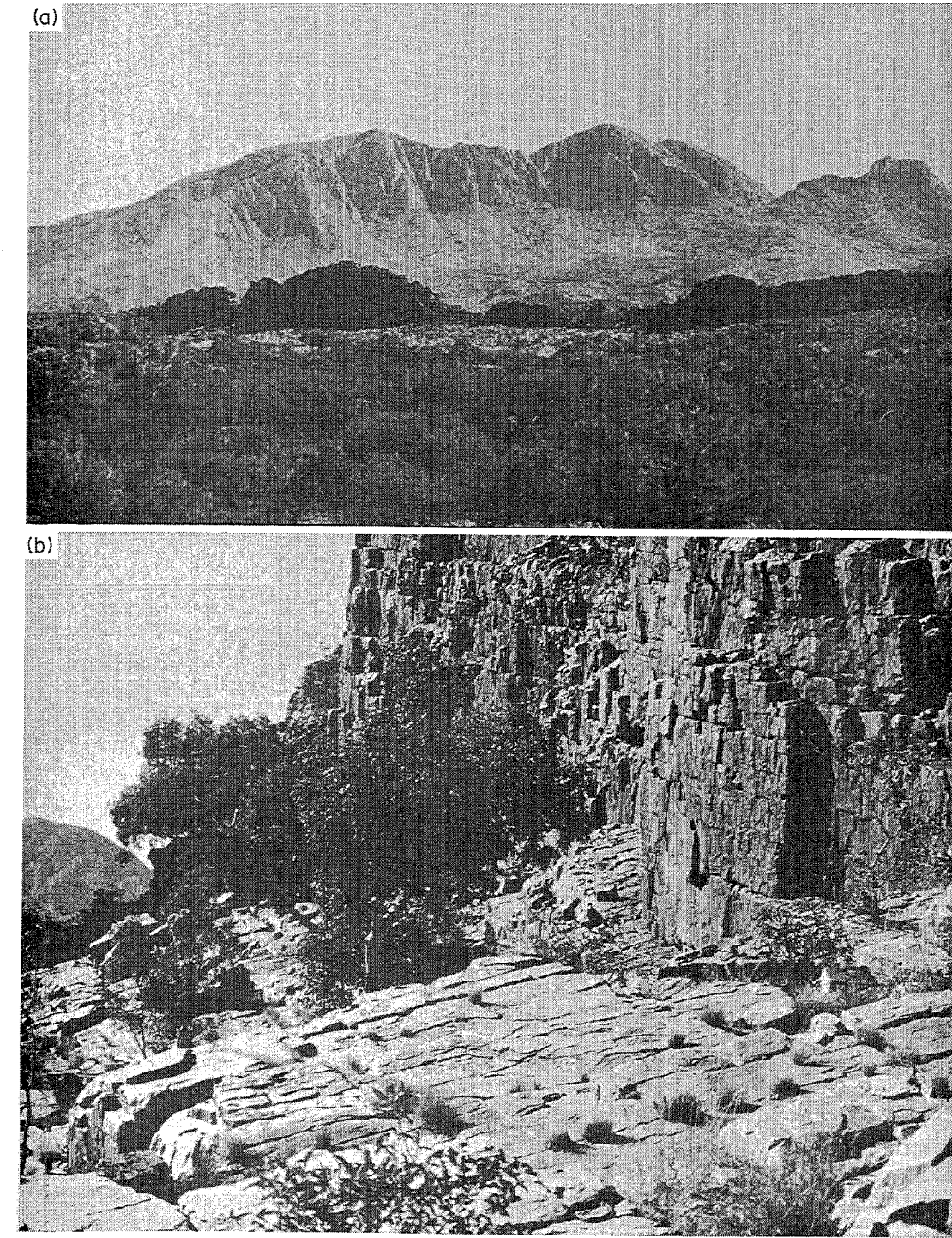


Figure 9a, b

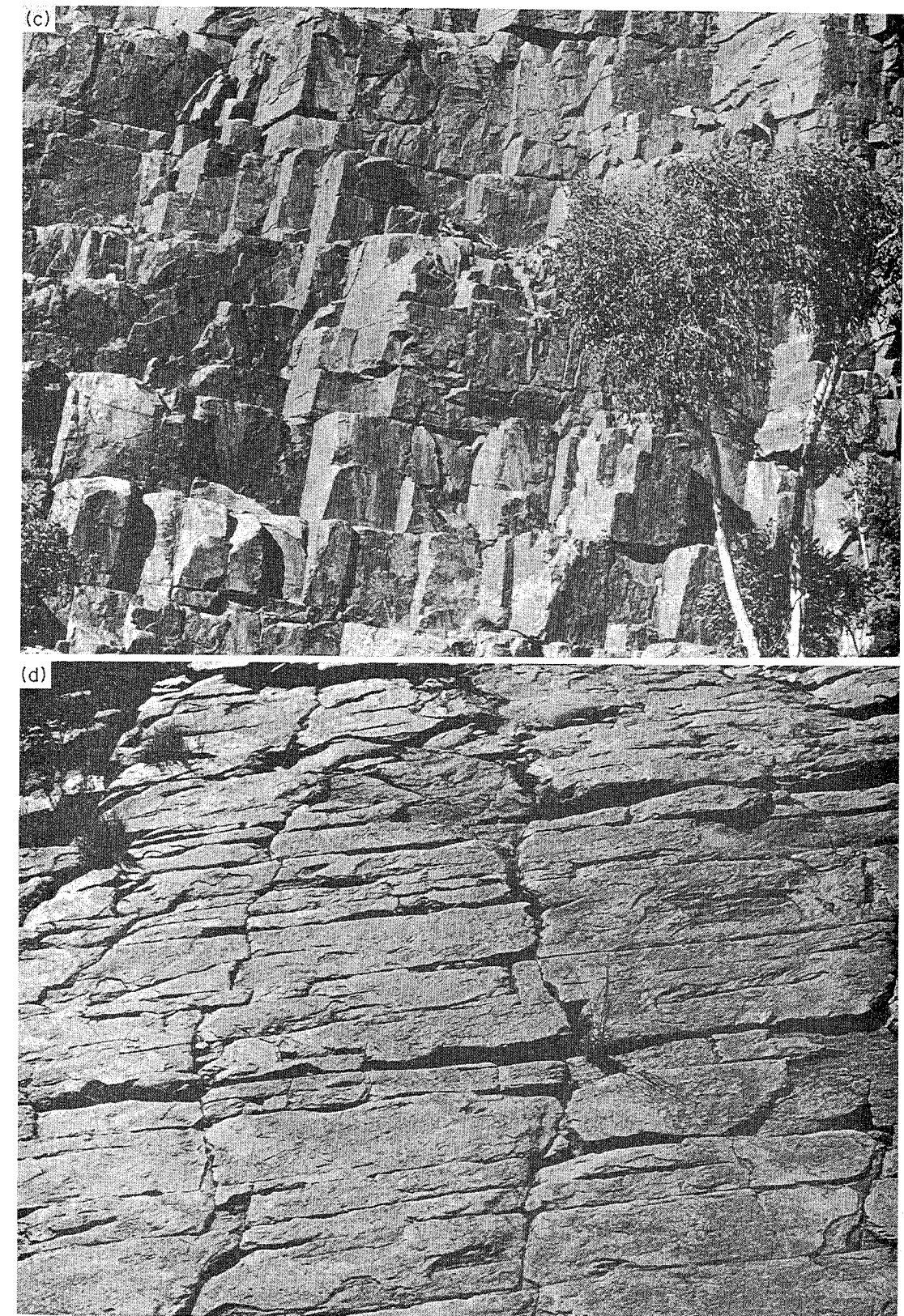


Figure 9 Jointing at various scales in Heavitree Quartzite, Central Australia. (a) Mount Sonder, (b)–(d) Ormiston Gorge

a scale is not included one commonly cannot guess the absolute size of the structure being photographed. One can express this second observation by saying that many structures in deformed rocks possess scale invariance in their overall patterns of spatial development.

The purpose of this chapter is to emphasize that these two observations concerning discontinuities, namely, an element of irregularity that suggests description in terms of statistical parameters and scale invariance are the hallmarks of the fractal nature of these structures. If one views discontinuities as fractal structures then their irregularities and somewhat erratic orientation patterns and spatial distributions are seen as resulting from very well defined rules of fractal geometry that have their origins in well founded physical laws. The irregularity and the scale invariance follow directly from the physical processes that form discontinuities during deformation of the rock mass; the irregularity and the scale invariance are not nondeterministic quirks of Nature, they arise from well defined laws of Nature and are in fact what Nature is all about!

Studies of discontinuity orientation and spacing and of block size and shape are commonly complicated by the great diversity of orientations, spacings and persistence of discontinuities within the rock mass (Figure 10). In order to make some sense of these observations, workers will commonly smooth data, or adopt some form of 'window' approach, or resort to some form of statistical representation (such as 'mean' values) of orientation, spacing, persistence or block size. This leads to much data being thrown away and to some form of idealized representation being adopted that may or may not be a good representation of reality depending on how much smoothing has taken place. In this section it is emphasized that diversity of orientation, spacing and persistence is an intrinsic part of discontinuity development and should be accepted as part of the description of any rock mass. Moreover there are elegant and concise ways of quantifying this diversity and irregularity in terms of fractal geometry.

### 2.3.2 Nonlinear Dynamics and Fractal Geometries

Irregularity is the hallmark of geological structures (see Figure 11); many show quasiperiodicity yet are irregular enough that it is difficult to make predictions where the next fold hinge, shear zone or major joint plane will be within a system of such structures. One of the fundamental problems in structural geology, within the context of rock mechanics, is to make such predictions with a considerable degree of certainty (see Section 2.7).

It is now known that systems far removed from equilibrium are capable of undergoing internal rearrangements to produce quasiordered structures under the action of relatively small perturbations [47]. The prerequisites for such ordering in three dimensions are: that the system should have three or more independent degrees of freedom which in turn implies that the system is governed by three or more differential equations; that these differential equations should describe nonlinear relations; and that there should be strong feedback mechanisms in operation between the processes described by these equations.

Most geological structures in deformed rocks owe their existence to feedback interactions between a minimum of three differential equations: (i) the stress equations of motion (*i.e.* Newton's first law of motion); (ii) a yield equation which describes the conditions under which plastic or elastic deformation and unloading occurs; and (iii) a flow rule which describes the relation between the direction of plastic incremental strain and the stress.

In general other relationships are required such as those that describe strain softening, changes in volume or permeability with plastic strain, the way in which fluid flow is coupled to deformation, and the way in which mineral solution, transport and deposition are coupled to deformation.

One should suspect therefore, by analogy with other systems [47], that self-organization should be a prominent behavior pattern in geological systems. However, to date there has been little formal treatment of such systems although notable exceptions include Cundall [48], Ord [49] and Mühlhaus [50].

The work of Cundall and of Ord will be considered in Section 2.7. For the present we concentrate on a summary of the work of Mühlhaus.

An outstanding problem in structural geology involves the buckling of an inelastic layer under compression and embedded in an inelastic medium. Published solutions to this problem in classical papers such as those of Biot [51] and Ramberg [52] predict the amplification of a single dominant wavelength no matter what spectrum of initial irregularities exists in the layer. The result is that strictly periodic fold structures should always develop.

Mühlhaus has shown the following.

(i) Geometrical nonlinearities are generally too small to account for the development of aperiodic structures.



Figure 10 (a) Complicated jointing in Ieru Formation, Ok Tedi copper-gold mine PNG. (b) Complicated vein systems associated with copper mineralization, Hilton Mine, Queensland, Australia (Photo: Rick Valenta)

(ii) The nonlinear theory of large amplitude folding predicts that even for a white noise initial distribution of amplitudes, after a short time, the appearance of the fold is governed by the fastest growing mode; for longer times a much broader distribution of amplitudes is amplified leading to an irregular geometry which is aperiodic.



Figure 11 Vein systems, Banff, Canada

(iii) The nonlinear theory of large amplitude folding is formally similar to the theory for spinodal decomposition; thus there is a rational explanation for the similarity between the spatial distribution of concentration in the spinodal region and fold amplitude patterns.

(iv) The classical Biot and Ramberg treatments consider only the normal stresses acting within a layer and neglect the layer parallel shear stresses; it is these shear stresses which contribute to the nonlinearity of the problem with the resultant development of irregular geometries.

Thus, the ingredients are present within the mathematical formalities to indicate why the development of erratic structures should be the norm in structural geology rather than strictly periodic structures and one can only await future developments in this exciting field.

Meanwhile, analogy with other nonlinear systems suggests, given the equations governing the development of geological structures, that quasiperiodic or erratic geometries should be well developed as is indeed observed (see Figure 12).

In the subsequent sections we show that suitable systems of affine transformations with feedback mappings of one affine transformation into another are capable of duplicating the irregularities characteristic of geological structures. It can only be supposed, at this primitive stage in the development of the subject, that these affine transformations are first order approximations to the solutions of the governing mechanical equations in state space. The feedback involved in the mappings, it will be shown, is fundamental to the development of fractal geometries and this in some way must be analogous to the dynamic feedback and interaction which exists between various parts of inhomogeneously deforming bodies [48].



Figure 12 Fold system, quartz-schist, Central Australia

### 2.3.3 Fractals and Fractal Dimension

Surprisingly, although the literature on fractals is now immense, there appears to be no published definition of the term fractal, except in Feder [53]. Feder reports that a commonly quoted, but somewhat opaque definition, namely, 'a fractal is by definition a set for which the Hausdorff-Besicovitch dimension strictly exceeds the topological dimension' [54] has been retracted by Mandelbrot and instead the following substituted: 'a fractal is a shape made of parts similar to the whole in some way'.

We elaborate upon this latter definition: a fractal can be thought of as an array of points which constitutes a subset of a particular space of interest. Examples of fractals of interest in geomechanics are the trace of a joint on another two-dimensional surface, the array of points that constitutes a joint surface embedded within three-dimensional Euclidean space, the array of points that comprises a complicated set of joints embedded within a three-dimensional Euclidean space or the array of points that constitutes the orientation diagram for poles to joints embedded in the Riemannian surface of a sphere.

The presence of structure over many orders of magnitude in scale is one of the hallmarks of fractal geometry. This means that fractals are scale invariant over some range in scale although it is important to distinguish between self-similar and self-affine fractal geometries when considering scale invariance. A self-similar fractal appears geometrically similar over some range of magnifications (or dilations); a self-affine fractal appears similar over a range of magnifications except that the fractal needs to be stretched differently in two orthogonal directions and/or sheared in order to generate strict geometrical similarity at various scales. The power spectrum for a self-similar surface has a slope of  $-2$ , whereas that for a self-affine surface has a slope of  $-3$  [55]. Many natural joints appear to be self-affine, whereas some natural faults are self-similar in their surface geometry [55].

A fractal is characterized by a number,  $D$ , which describes how densely the subset occupies the space in which it lies;  $D$  is independent of the units of measurement and can have a value between or equal to the topological dimension of the subset and the dimension of the space in which the subset is embedded. There is no need for  $D$  to be fractional in value; it can take on integer values.

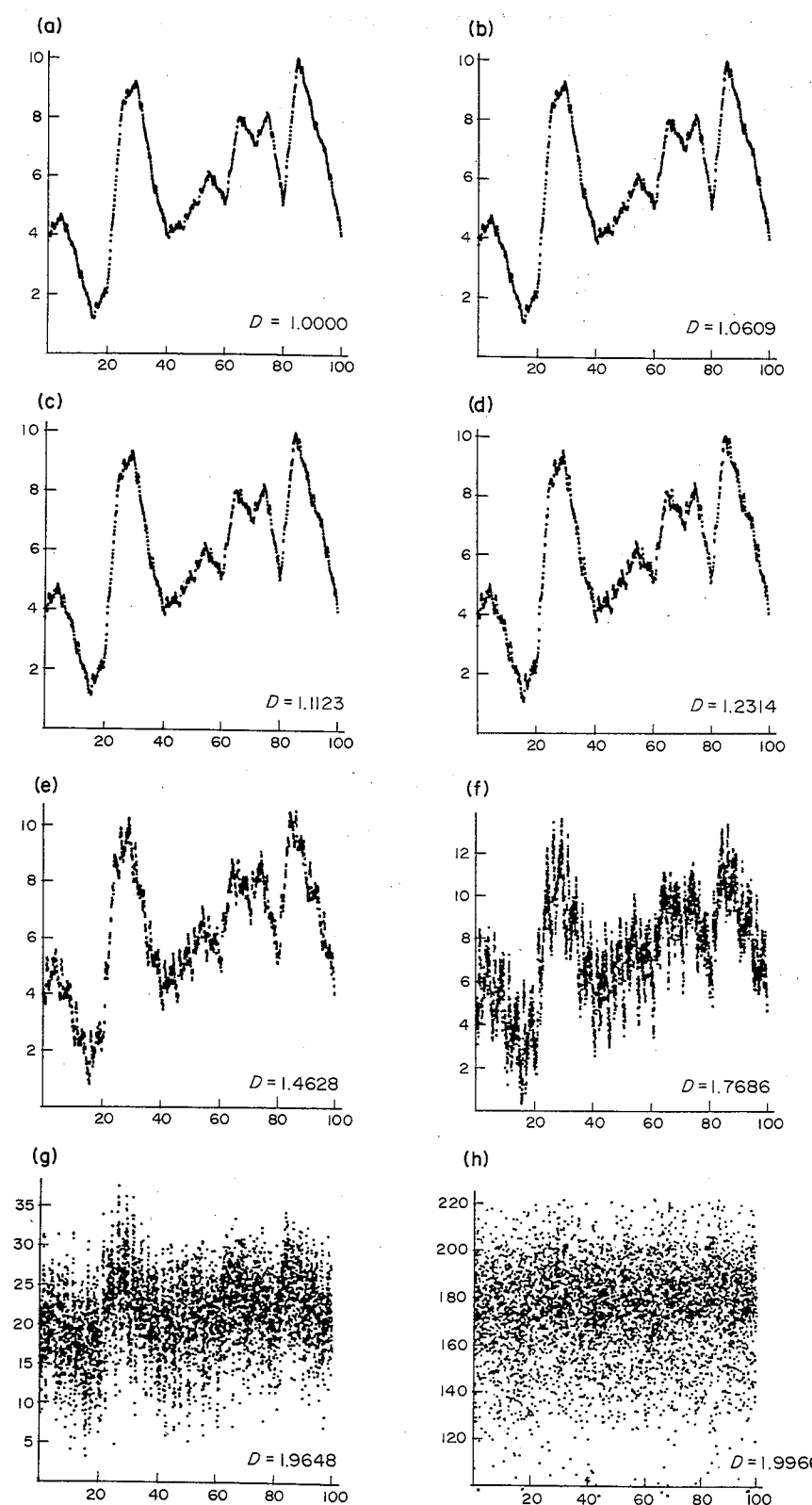


**Figure 13** Fractal interpolation fit to the classical Barton and Choubey [6] joint profile with JRC = 18–20 (vertical scale exaggerated). (a)  $D = 1.0000$ , (b)  $D = 1.0609$ , (c)  $D = 1.1123$ , (d)  $D = 1.2314$ , (e)  $D = 1.4628$ , (f)  $D = 1.7686$ , (g)  $D = 1.9648$ , (h)  $D = 1.9966$

Figure 13 is presented to give some feeling for fractal geometry. The method of calculating Figure 13 is presented in Section 2.3.5. Figure 13(a) shows a set of points which define a joint trace with a JRC lying between 18 and 20. This trace is in fact the classical trace portrayed by Barton and Choubey [6], but with the vertical scale exaggerated. The fractal dimension of the set represented in Figure 13(a) is equal to one which is identical to the topological dimension. The subsequent parts of Figure 13 show a progressive 'roughening' of the classical Barton joint trace as the fractal dimension increases from  $D = 1.0609$  in Figure 13(b) to  $D = 1.9966$  in Figure 13(h). As the fractal dimension increases from one towards two, the set of points tends to fill the two-dimensional Euclidean space more and more densely.

It is important to note that the distribution of points in Figure 13 is not random. Consider for example Figure 13(h) for which  $D = 1.9966$ . There are 5000 points plotted in Figure 13(h); 20 000 points are plotted in Figure 14(a) for  $D = 1.9966$  and, as is to be expected for a fractal dimension close to 2.0, the points continue to approximate a space of dimension two. However, the distribution is not random and an expansion of the scale as in Figure 14(b) continues to show quite definite structure. A random distribution of points would tend to uniformly occupy the two-dimensional space for large numbers of points with no fine structure. The fractal shown in Figures 13(h) and 14 never fills the two-dimensional plane more densely than is shown, no matter how many new points are added to the set.

For both self-similar and self-affine fractals, the fractal dimension,  $D$ , of the fractal may be established by finding the smallest number,  $N(\varepsilon)$ , of balls of radius  $\varepsilon$ , that are needed to cover the fractal. Thus, for a range of radii,  $\varepsilon$ , that fractal is said to possess a fractal dimension,  $D$ , if

$$N(\varepsilon) = C\varepsilon^{-D} \quad (1)$$

for a positive constant,  $C$ .

In practice, square boxes are generally used in order to determine  $D$  for a fractal, in place of balls [56, 57].

### 2.3.4 Affine Transformations and Iterated Function Systems (IFS)

Deterministic fractal geometry is concerned with those subsets of space which are generated by simple geometrical transformations of the space into itself [58].

In what follows we work only in two-dimensional Euclidean space; extension to three-dimensional Euclidean space or to the surface of a sphere is straightforward. Simple examples of such transformations are affine transformations of the kind

$$w(x_1, x_2) = \begin{bmatrix} a_{11} & a_{12} \\ a_{21} & a_{22} \end{bmatrix} \begin{bmatrix} x_1 \\ x_2 \end{bmatrix} + \begin{bmatrix} t_1 \\ t_2 \end{bmatrix}$$

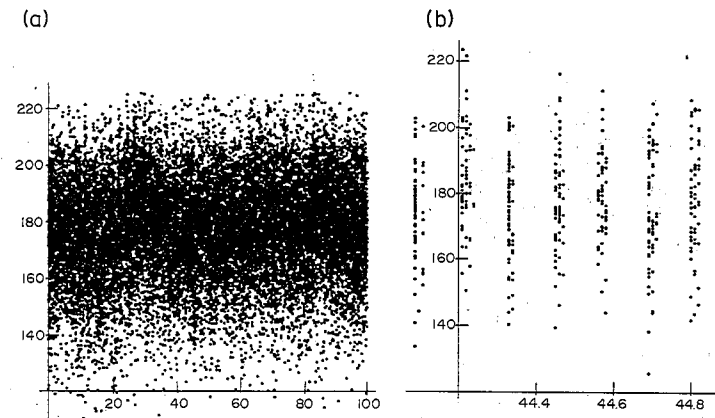


**Figure 14** (a) Same as Figure 13(h) but with 20 000 points plotted, as opposed to 5000 in Figure 13(h); (b) detail of structure in (a)

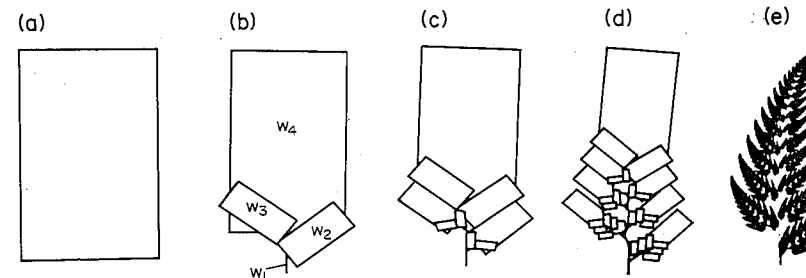


Figure 17 Example of a tiling process that ultimately produces a fern (after Jurgens *et al.* [60])

and such that  $p_n$  is always greater than zero. This means that each  $p_n$  is proportional to the area of the parallelogram which arises when a unit square is transformed by  $w_n$ .

The operation of the IFS produces a fractal attractor.

The coefficients of an IFS are conveniently represented in a table containing the  $a_{ij}$  and  $t_i$  of expression (2) and which constitutes the IFS code.

An alternative and highly useful way of thinking about IFSs is summarized by Figure 17. Figure 17(b) shows four affine transformations which are represented by the four parallelograms labeled  $w_1, w_2, w_3, w_4$ . Iteration of these transformations in the manner discussed above results in progressive refinement of the attractor until finally the fractal form shown in Figure 17(e) is produced [60]. The important point here is that the transformations required to produce the final fractal attractor can be found by 'tiling' a relatively small number of parallelograms, representing transformations, over the attractor. This latter statement is an expression of the Collage Theorem [59] which states that any fractal can be reproduced by first tiling a series of parallelograms over the fractal. The array of parallelograms then represents an IFS which can be used to generate the fractal.

An IFS consisting only of similitudes with no inversions (that is, the transformations are of the form of equation 3) leads to a self-similar fractal. An IFS consisting of similitudes with an inversion (that is, transformations of the form of equation 4) leads to a self-inverse fractal. Otherwise the fractals generated by IFSs are self-affine.

Notice, however, that it is possible for fractals to exist which are combinations of self-similar and self-affine fractals. An example is given in Figure 18 where the word JOINT is generated as a fractal using the 15 affine transformations represented in Figure 18(a). The fractal in Figure 18(b) has repeated structure on finer and finer scale so that no matter how much the figure is magnified the word JOINT is always apparent (Figure 18c). Parts of the fractal (such as the crossbar on the J) are self-affine fractals with no shear; other parts (such as the diagonal on the N) are self-affine fractals with shear; other parts (such as the dot on the I) are self-similar fractals. The creation of the fractal JOINT using the transformations shown in Figure 18 is an example of the use of the Collage Theorem.

### 2.3.5 Fractal Interpolation Functions

Barnsley [59] shows that any curve such as the one shown in Figure 19 can be reproduced by a set of transformations of the form

$$w_n \begin{pmatrix} x_1 \\ x_2 \end{pmatrix} = \begin{pmatrix} a_{11} & 0 \\ a_{21} & a_{22} \end{pmatrix} \begin{pmatrix} x_1 \\ x_2 \end{pmatrix} + \begin{pmatrix} t_1 \\ t_2 \end{pmatrix} \quad (5)$$

for

$$n = 1, 2, \dots, (N - 1)$$

where  $N (> 1)$  is the number of data points on the curve represented by the series of coordinates  $(X_1^1, X_2^1), (X_1^2, X_2^2), \dots, (X_1^N, X_2^N)$ . Here, the  $a_{22}^{(n)}$ s are known as vertical scaling factors and obey  $0 \leq a_{22}^{(n)} < 1$ ; they are selected in order to control the fractal dimension or the 'roughness' of the

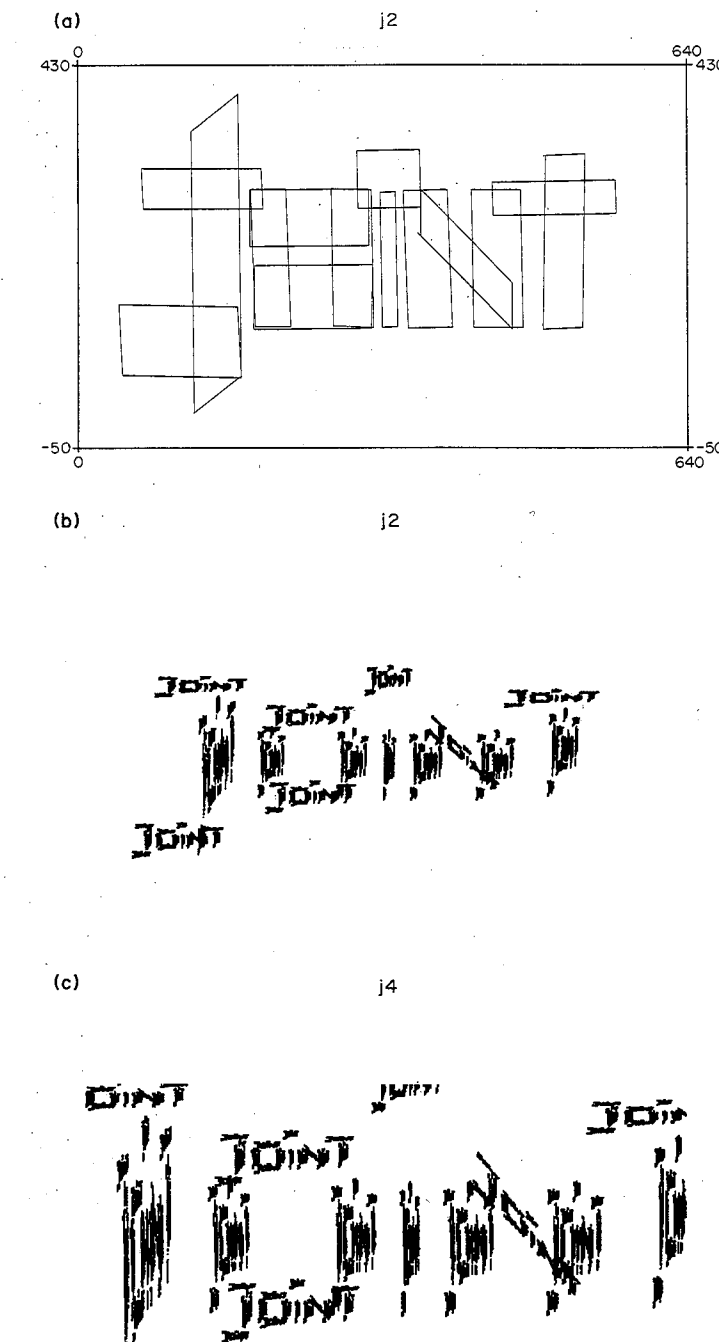


Figure 18 (a) Tiling for the word JOINT; (b) Fractal resulting from the transformations shown in (a); (c) Zoom on the cross bar over the J in (b)

curve as indicated below. The constants  $a_{11}^{(n)}, a_{21}^{(n)}, t_1^{(n)}$  and  $t_2^{(n)}$  are defined by

$$\begin{aligned} a_{11}^{(n)} &= (X_1^{(n)} - X_1^{(n-1)})/B \\ a_{21}^{(n)} &= (X_2^{(n)} - X_2^{(n-1)})/B - a_{22}^{(n)}(X_2^{(N)} - X_2^{(1)})/B \\ t_1^{(n)} &= (X_1^{(N)} X_1^{(n-1)} - X_1^{(1)})/B \\ t_2^{(n)} &= (X_1^{(N)} X_2^{(n-1)} - X_1^{(1)})/B - a_{22}^{(n)}(X_1^{(N)} X_2^{(1)} - X_1^{(1)} X_2^{(N)})/B \end{aligned} \quad (6)$$

where  $B = (X_1^{(N)} - X_1^{(1)})$ .

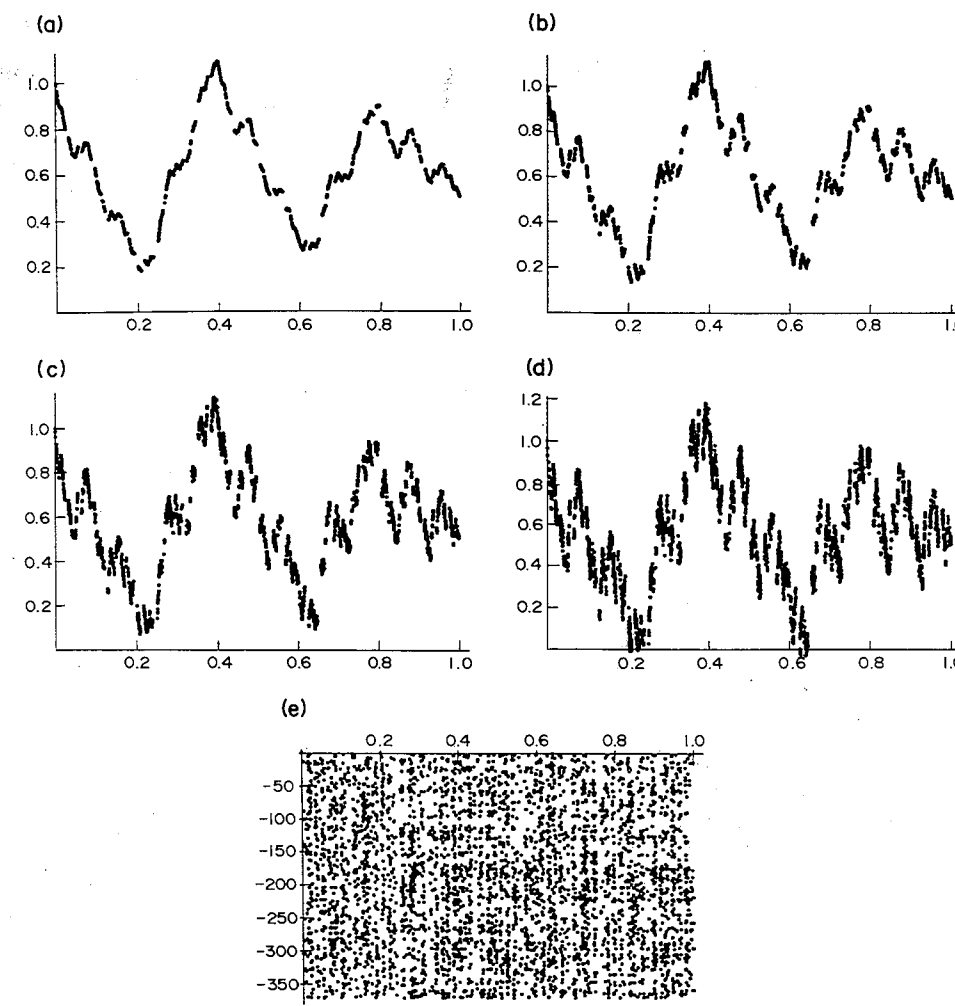


Figure 19 Fractal interpolation fits to the data points  $(0.0, 1.0), (0.2, 0.2), (0.4, 1.1), (0.6, 0.3), (0.8, 0.9), (1.0, 0.5)$ . (a)  $D = 1.00$ , (b)  $D = 1.25$ , (c)  $D = 1.43$ , (d)  $D = 1.57$ , (e)  $D = 2.00$

If

$$\sum_{n=1}^N |a_{22}^{(n)}| > 1$$

and the data points do not define a single straight line, then the fractal dimension of the curve which is generated by equation (5) is given by the unique real solution of

$$\sum_{n=1}^N |a_{22}^{(n)}| (a_{11}^{(n)})^{D-1} = 1 \quad (7)$$

otherwise the fractal dimension of the curve is one.

An example has been presented in Figure 13 and another is presented in Figure 19 where a curve is shown passing through the points whose coordinates are  $(0.0, 1.0), (0.2, 0.2), (0.4, 1.1), (0.6, 0.3), (0.8, 0.9)$  and  $(1.0, 0.5)$ . The resultant curve generated by the fractal interpolation procedure is shown in Figure 19(b) for chosen values of  $a_{22}^{(n)}$  given by  $a_{22}^{(1)} = a_{22}^{(2)} = a_{22}^{(3)} = 0.3$ . This gives a fractal dimension for the curve of  $D = 1.25$ . Figures 19(c), (d) and (e) show fractal curves fitting the same series of points but with fractal dimensions of 1.43, 1.57 and 2.0, respectively. Clearly, by this process it is possible to generate a joint trace of any complexity and with a given fractal dimension.

## 2.4 FRACTAL REPRESENTATION OF THE PROFILES OF SINGLE JOINTS AND OF JOINT ROUGHNESS

### 2.4.1 Fractal Representation of Profiles

In Section 2.3.5 it has been shown that fractal interpolation functions may be used to reproduce the profile of any joint surface to any required degree of accuracy [59]. There has been much discussion in the literature in an attempt to establish a correlation between joint roughness and fractal dimension and this is discussed in some detail in Section 2.4.2. There is no doubt that for design purposes it would be convenient to represent the profile of a joint by a single number such as  $D$  and this has been the motivation behind recent work. The purpose of this section is to point out that such a simple correlation is unlikely and that more than just the fractal dimension is required in order to characterize a joint profile.

The previous discussion on fractal interpolation functions indicates that the fractal dimension of any joint profile can be generated by these procedures. However, the shape of a particular joint profile is clearly characterized by more than just a fractal dimension and both  $C$  and  $D$  in expression (1) are necessary.

It remains to be seen if there is any correlation between  $C$ ,  $D$  and the mechanical properties of joints, but as yet no such experimental work has been carried out.

### 2.4.2 Joint Roughness

The importance in distinguishing between self-similar and self-affine fractals is brought out by considering fractals such as the profiles of joint surfaces that topologically have a dimension of one and are embedded in two-dimensional Euclidean space. One method of determining the fractal dimension of a curve is to use a pair of dividers and step off the distance along the curve. Using different opening distances,  $\epsilon$ , for the dividers for successive determinations of the length of the curve, an expression similar to equation (1) may then be used to determine  $D$ . For a self-similar fractal, the divider method always gives the correct value for  $D$  (subject to the practical limitations discussed by Pruess, [57]). However, for a self-affine fractal, important practical problems arise in determining  $D$  by the divider method (see Brown [61]; Power *et al.* [55]). Since the divider method has been used extensively in geomechanics literature recently, it is worth repeating the essential features of the problems associated with self-affine fractals here.

Consider a self-affine fractal embedded in two-dimensional Euclidean space and with a nominal length  $\lambda_0$ ; suppose that the fractal has been digitized at a number of points of equal spacing  $r$ . The vertical height fluctuations in the fractal over the distance  $r$  are, on average, equal to the standard deviation,  $\sigma$ , of the heights over the nominal length of the fractal. There are  $\lambda_0/r$  segments defining the fractal so that the length of the fractal is approximately

$$\lambda = \frac{\lambda_0}{r} \{r^2 + \sigma^2\}^{1/2} \quad (8)$$

Wong [62] has shown that for a self-affine fractal, over a distance  $r$ , the standard deviation of heights is  $\sigma = b(r/b)^{2-D}$  where  $b$  is a quantity known as the crossover distance. Thus, expression (8) becomes

$$\lambda = \lambda_0 \left\{ 1 + \left( \frac{r}{b} \right)^{2(1-D)} \right\}^{1/2} \quad (9)$$

For  $r \ll b$ , expression (9) becomes  $\lambda \approx \lambda_0(r/b)^{1-D}$  and so  $D$  may be obtained directly from a plot of  $\log(\lambda)$  against  $\log(r)$ , where the slope is  $(1-D)$ . However, for  $r \gg b$ ,  $\lambda \approx \lambda_0$  and we obtain  $D_{\text{apparent}} \approx 1$ . Brown and Scholz [63] estimate the crossover length to be in the range  $10^{-8}$  to  $10^{-5}$  m for natural joints, so that unless one has very fine resolution on the joint surface (better than a small part of a millimeter horizontally) then the divider length,  $r$ , is always much larger than the crossover length and one expects to see apparent fractal dimensions close to 1.0. For instance Lee *et al.* [64] report fractal dimensions for natural joints in the range 1.000107 to 1.021994. These results are considered in greater detail below.

The work of Barton and his coworkers (see for instance Barton [65]; Barton and Choubey [6]; Barton [66]; Barton and Bandis [67]) has established clear empirical relations between the shear strength of a particular rock joint and its roughness as measured by the Joint Roughness Coefficient. The JRC is determined in a somewhat subjective manner by comparing the profile of a joint with a standard set of joint profiles in which the JRC varies from 0 at the smoothest to 20 at the roughest. Various authors (including Turk *et al.* [68]; Carr and Warriner [69]; Carr [70–72]; Lee *et al.* [73]) have attempted to draw correlations between the fractal dimensions of joint surfaces and JRC, the intention being to develop a quantitative method of specifying joint roughness. A fractal approach would be of added importance in that it would enable scale effects on joint roughness to be considered.

The existing work on correlating JRC with the fractal dimensions of surfaces suffers from the following three limitations which need to be addressed before the results can be accepted as a basis for design work.

(i) The reference diagrams for JRC (such as Figure 8 of Barton and Choubey [6]) are essentially Euclidean curves with no roughness detail finer than about the line thickness. In other words, these reference curves are essentially nonfractal in character although the joint surfaces they were derived from undoubtedly have roughness detail much finer than has been portrayed in print (see for example the detail presented by Power and Tullis [74]). This means that any attempt to define fractal dimensions for the standard JRC curves must produce values for  $D$  exactly coinciding with the topological dimension of one. In a similar vein, any attempt to fit a fractal interpolation function to the published JRC curves also results in  $D = 1.0$  exactly. This can be seen immediately from expression (7) and the discussion which surrounds this expression. If we use 20 equally spaced points to fit a fractal interpolation function to the  $JRC = 18\text{--}20$  curve of Barton and Choubey [6] then  $a_{11} = 1/20$  for all  $w_n$ . Examination of Figure 13 shows that for all  $a_{22}^{(n)} > 0.05$  the resulting surface is far too rough and in fact  $a_{22}^{(n)} = 0.05$  ( $n = 1, 2, \dots, 20$ ) produces a surface which is marginally too rough to reproduce the published curve. Thus,  $\sum_{n=1}^{20} |a_{22}^{(n)}| \leq 1$  and hence  $D = 1$  exactly for all curves that come close to reproducing the published curve.

(ii) The joint profiles published by Barton and Choubey represent joints which are self-affine in character. That these joints are self-affine is self evident since they have roughness when viewed on a fine scale yet approximate Euclidean two-dimensional surfaces when viewed at a coarse scale. As such, unless the resolution of the divider or box-counting method is finer than the crossover distance as defined by Wong [62] and by Brown [61], then an apparent fractal dimension is produced which must be close to one in value. This is in fact what is produced by workers who have published in this area and results solely from the fact that the resolution of the counting algorithm is far coarser than the finest detail on the surface of the joint.

(iii) Determination of the fractal dimension of a fractal set to high precision is by no means a straightforward task and Pruess [57] has recently discussed some of the problems involved. Pruess shows that even for sets where the fractal dimension is precisely known, it can be difficult to arrive at the known value of  $D$  unless the values of  $\epsilon$  in expression (1) are strategically selected. In view of the above remarks on precision, values of  $D$  that are quoted to six decimal places (see Lee *et al.* [73]) have to be supported with a rigorous analysis of the way in which  $D$  varies with the measurement procedure.

These three limitations mean that published correlations of JRC with  $D$  must be justified with further work if they are to be accepted. In particular, there is little value in attempting a correlation with published curves unless detail is reproduced to a very fine scale; work generally has to involve the actual joint surfaces and care has to be taken to ensure that roughness detail is resolved on a scale smaller than the crossover distance. It seems that as yet there is no case for a correlation between JRC and the fractal dimension of a surface.

The above conclusions are emphasized by the recent work of Miller *et al.* [75] who highlighted the difficulties associated with obtaining meaningful measures of  $D$  for surface profiles. Brown [61] has pointed out that two parameters are needed to specify the roughness of a profile if a fractal approach is taken: one of these is the fractal dimension,  $D$ , and the other is a measure of the amplitude of the surface at a particular wavelength. It is this latter parameter which is more likely to correlate directly with visual estimates of surface roughness as concluded by Miller *et al.* [75].

Above all, because of the anisotropy and the inhomogeneity of roughness on many discontinuities it seems rather pointless to seek correlations between mechanical properties and 'surface roughness' parameters derived from a single profile. Rather, effort should be devoted to measuring the fractal dimensions of surfaces together with some measure of the amplitude at a reference wavelength and attempting some correlation between these measures and mechanical properties rather than working with single profiles across these surfaces.

## 2.5 JOINT SYSTEMS

### 2.5.1 Simple Joint Sets

#### 2.5.1.1 The statistical approach to discontinuity geometry

Since the geometry of discontinuities in rock masses is clearly very irregular (stochastic is a term commonly used) it has been natural to apply statistical methods to the description and modeling of this geometry. In a series of papers [42, 76, 77], Hudson and Priest have represented discontinuity geometry in two dimensions as an array of randomly distributed lines. Hudson and Priest point out that a random distribution implies that the spacing of joints belonging to a particular set of discontinuities (all approximately parallel in orientation) is

$$f(l) = \lambda \exp(-\lambda l) \quad (10)$$

where  $f(l)$  is the frequency of spacing,  $l$ , and  $\lambda$  is a constant characteristic of the particular geometry. Expression (10) is commonly referred to as the negative exponential distribution.

Many natural discontinuity systems [42, 76] show spacing distributions which approximate closely to equation (10) although some workers have documented distributions which are log-normal [78]; others have suggested that a Weibull distribution may be applicable [79].

The various suggestions are the result of empirical 'curve-fitting' since, as yet, there is no theoretical basis in mechanics for suggesting one distribution in favor of another. As indicated, only the negative exponential distribution (equation 10) has any conceptual basis in that a random spatial distribution of lines means that spacings must follow a Poisson frequency distribution which, in turn, implies a distribution of the form of equation (10) [42].

There is an implication in much of the literature that a fractal set of joints in two dimensions must produce a spacing distribution which is identical to expression (10) [80]. Thus, if  $l$  is the spacing between joints then a spacing frequency distribution function of the form

$$p(l) = Al^{-D} \quad (11)$$

is postulated where  $(l)$  represents the frequency of joints with spacing greater than  $l$ .

It should be noted, however, that in two dimensions, expression (1) is an expression that describes the scaling law for the distribution of points which comprise the fractal in the plane. There is no inherent reason why expression (1) should describe the spacing between joints since that expression refers to the total fractal and not just one aspect of it. Thus, expression (11) is not a necessary or sufficient geometrical attribute of a fractal distribution of joints.

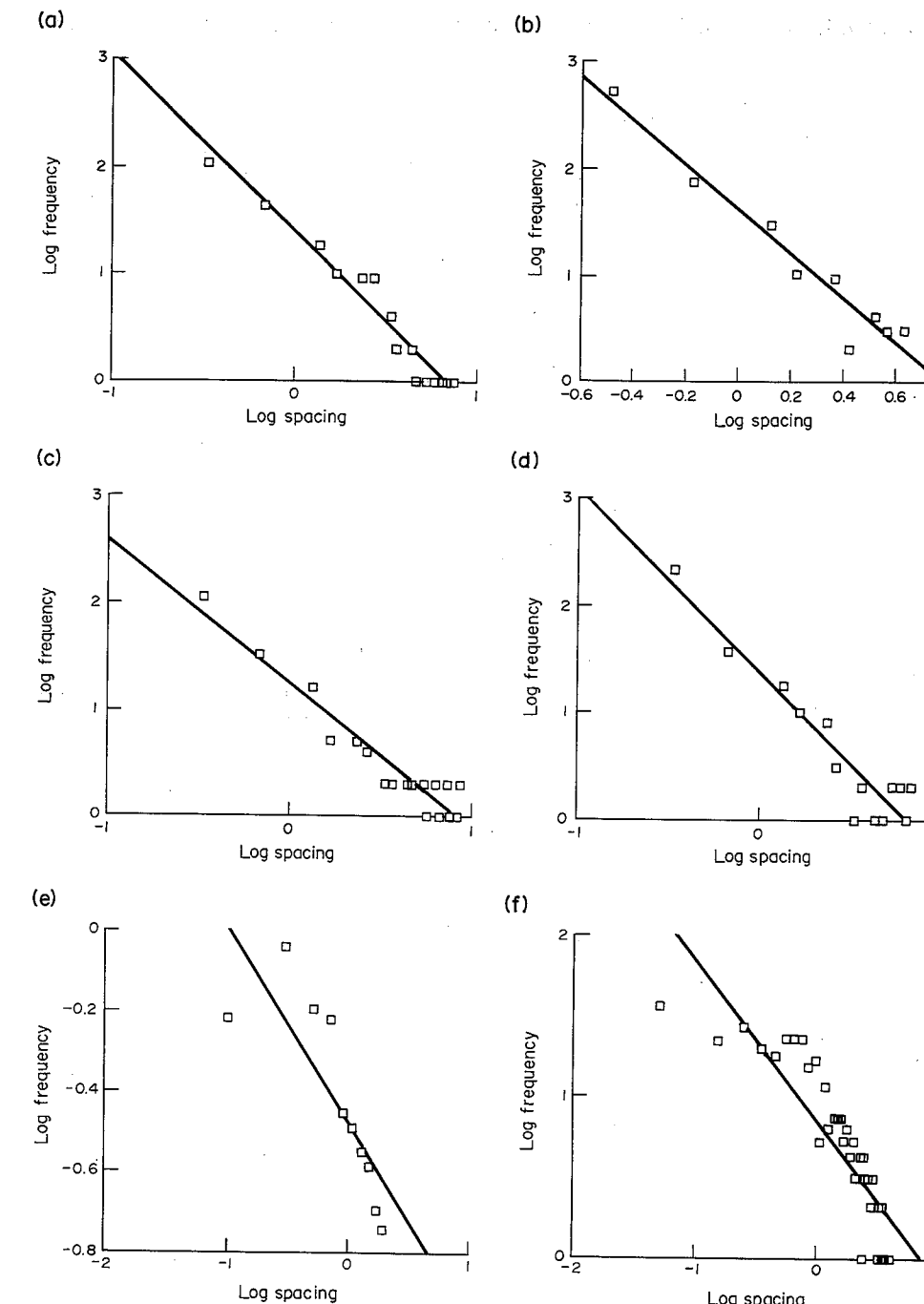
If we take the negative exponential distribution as a reference distribution then the log-normal distribution departs from the reference distribution in that there is a much greater proportion of small spacings than in the negative exponential distribution. The power law distribution is quite similar to the log-normal distribution over limited ranges. The Weibull distribution has an even greater proportion of small spacings than the log-normal distribution but both approach zero frequency as the spacing approaches zero. Thus discontinuity populations with a high proportion of small spacings relative to a random population might be expected to approximate to a log-normal or power law frequency distribution, whilst populations with an unusually high proportion of small spacings relative to a random distribution might be expected to approximate in part to a Weibull distribution.

Figure 20(a), (b), (c) and (d) shows some of the results of Roleau and Gale [78] for joint spacings in the Stripa Granite; they claim that a log-normal distribution is a good fit for the data. However, clearly a power law distribution has to be considered as well. Also shown in Figure 20 are joint distribution data taken from Hudson and Priest [42] and from La Pointe and Hudson [46] where negative exponential distributions are claimed. Here a power law distribution does not seem to fit the data very well.

Thus, any geometrical model of discontinuities in real rocks must show a tendency towards log-normal and power law frequency distributions for joint spacing. However, over limited ranges, particular joint sets, may show a tendency towards a negative exponential frequency distribution, whereas those joint sets with a relatively high frequency of small joint spacings may show a tendency towards a Weibull frequency distribution.

#### 2.5.1.2 Joint sets

Section 2.4 dealt with defining single joint profiles using fractal interpolation functions. This section is concerned with developing simple models for arrays of joints that possess all the



**Figure 20** Log-log plots for various published data sets. (a)–(d) Power law fit for Joint Sets 1–4, Stripa Granite [78]; the geometry of these joint sets is also adequately represented by a log-normal distribution [78]. (e), (f) Lack of power law fit to data published by Hudson and Priest [42, p. 360] and La Ponte and Hudson [46, p. 29] respectively; in both (e) and (f) the published data corresponds to a negative exponential distribution

characteristics of natural joints, namely an apparently irregular distribution of spacings that approximates a power law distribution, and variable orientations for a given set. In passing it should be noted that these models are also capable of producing power law, negative exponential, log-normal and Weibull frequency distributions for joint persistence as well.

We begin by examining some models that produce a fractal distribution of parallel straight joints and progress to more complicated distributions in Section 2.5.2.

A leading contender for a model for simple joint arrays is the  $N$ th-order Cantor Set defined by the IFS [59]

$$w_n(x_1) = \frac{1}{N+1} x_1 + \frac{n}{N+1}, \quad n = 1, 2, \dots, N \quad (12)$$

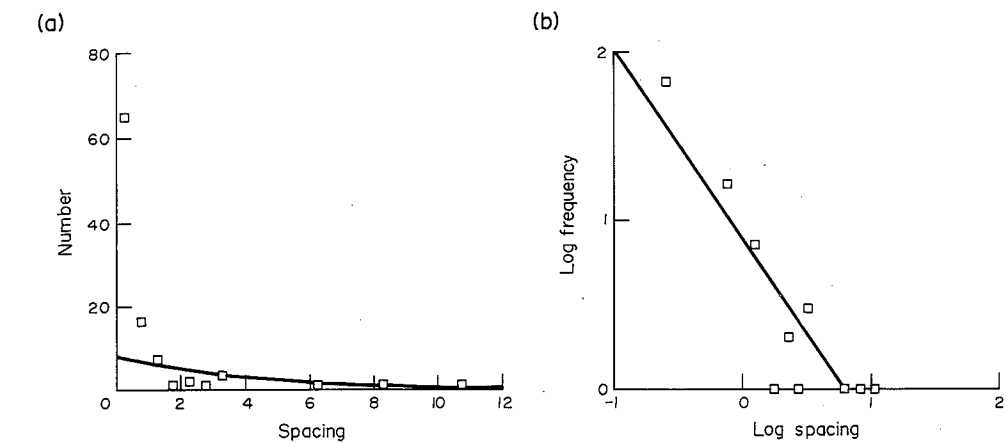


**Figure 21** (a) Lack of exponential distribution fit to data from third order Cantor Set, first 98 iterations. (b) Power law fit to data from third order Cantor Set, first 98 iterations

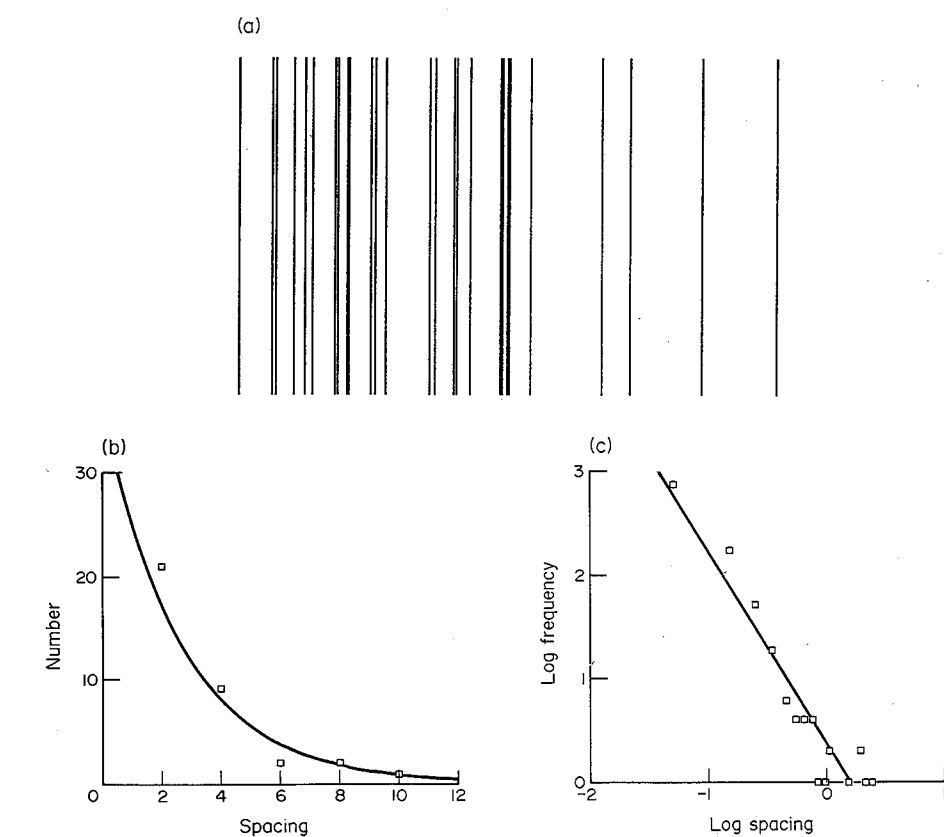


**Figure 22** (a) Geometry generated by first 30 iterations of the IFS represented by expression (13). (b) Exponential distribution fit to data generated by first 38 iterations of the IFS (5.4). (c) Power law fit to data generated by first 1000 iterations of the IFS (5.4)

The statistics of joint spacings arising from this IFS for  $N = 3$  are shown in Figure 21 in the form of plots of spacing *versus* frequency. A power law fits the data better than a negative exponential distribution. Some credence to the use of fractal distributions of the type used in Figure 21 is given by the work of Velde *et al.* [80] who use a Cantor's Dust method to examine the anisotropy of the spatial distribution of fractures.

An alternative fractal distribution of joints can be developed using the orbits of points that are produced in simple dynamical systems. An example is the IFS [59]

$$\begin{aligned} w_1(x_1) &= \frac{1}{2}x_1 \\ w_2(x_1) &= \frac{3}{4}x_1 + \frac{1}{4} \end{aligned} \quad (13)$$

The result of applying this IFS to an initial straight line parallel to  $x_2$  is given in Figure 22 together with details of the spacings generated.

For a small number of joints the IFS given in equation (13) results in an exponential frequency distribution (Figure 22b). For a large number of joints this same IFS gives a frequency distribution which can be well matched by a power law (Figure 22c).

## 2.5.2 Complicated Joint Systems

The previous discussion illustrated how simple joint systems can be generated using relatively simple IFSs. The resulting fractals comprise arrays of joints which are more or less parallel and

which themselves are linear. Below we introduce more complicated IFSs and demonstrate how realistic and complicated arrays of joints may be generated.

The basic principle adopted here is the tiling procedure illustrated in Figure 17. In that figure, the stem of the fern is produced by the affine transformation

$$w_1 = \begin{bmatrix} 0.0 & 0.0 \\ 0.0 & 0.17 \end{bmatrix} \begin{bmatrix} x_1 \\ x_2 \end{bmatrix} + \begin{bmatrix} 0.0 \\ 0.0 \end{bmatrix}$$

Here the shortening parallel to  $x_1$  is infinite so that the parallelogram representing the transformation appears as a straight line; its length is governed by the magnitude of  $a_{22}$  ( $=0.17$  in Figure 17).

Thus, any line segment can be generated by an affine transformation by giving suitable values to the  $a_{ij}$  in expression (2) and its position in space can be adjusted using the  $t_i$ . Some complexity (or 'damage') along the linear trace of a joint can be generated by opening the parallelogram representing the affine transformation a little; in Figure 17 this would mean making  $a_{11}$  in  $w_1$  small but nonzero.

Three examples are presented in Figures 23, 24 and 25 where a representation of the affine transformations is given together with the resulting fractal. In Figure 23 a single fractured zone is shown with 'pinnate' or 'feather' jointing developed. Figure 24 shows a more complicated joint system with two dominant joint sets developed; notice that all joints in a particular set are not strictly parallel and there is up to  $10^\circ$  scatter in the orientation of joints belonging to a particular set. In Figure 25 a joint system consisting of three dominant joint sets is shown with curvature of individual joints now being displayed.

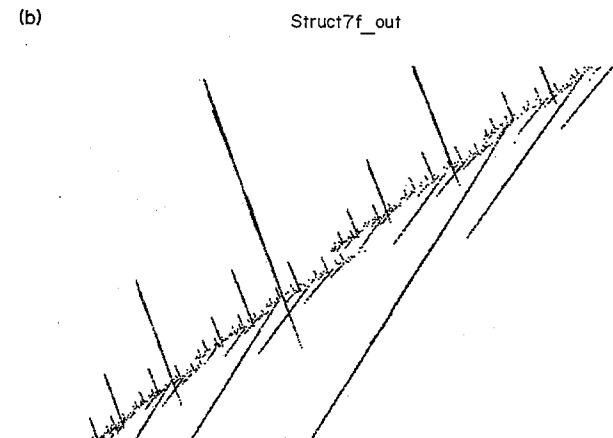
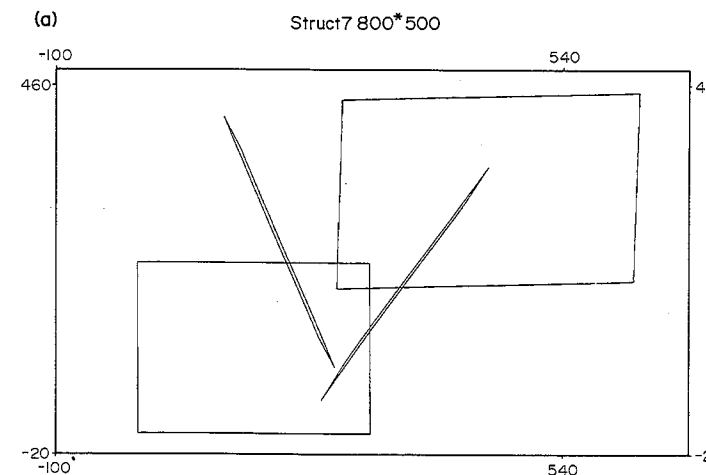


Figure 23 (a) Transformations representing the IFS which produces the fracture system shown in (b)

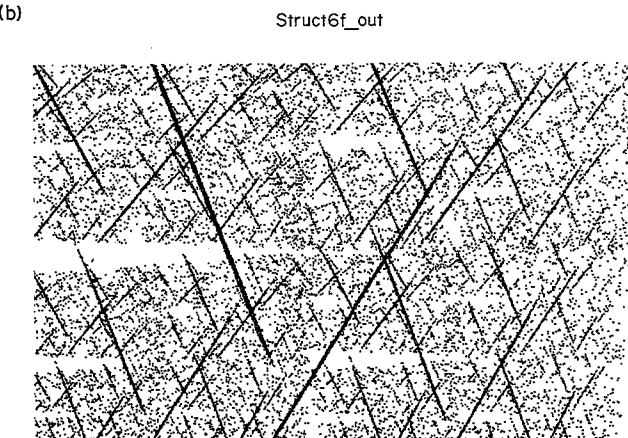
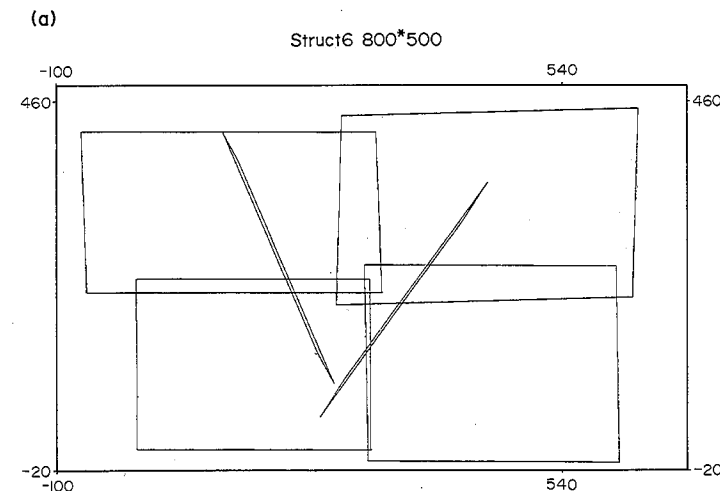


Figure 24 (a) Transformations representing the IFS which produces the joint system shown in (b)

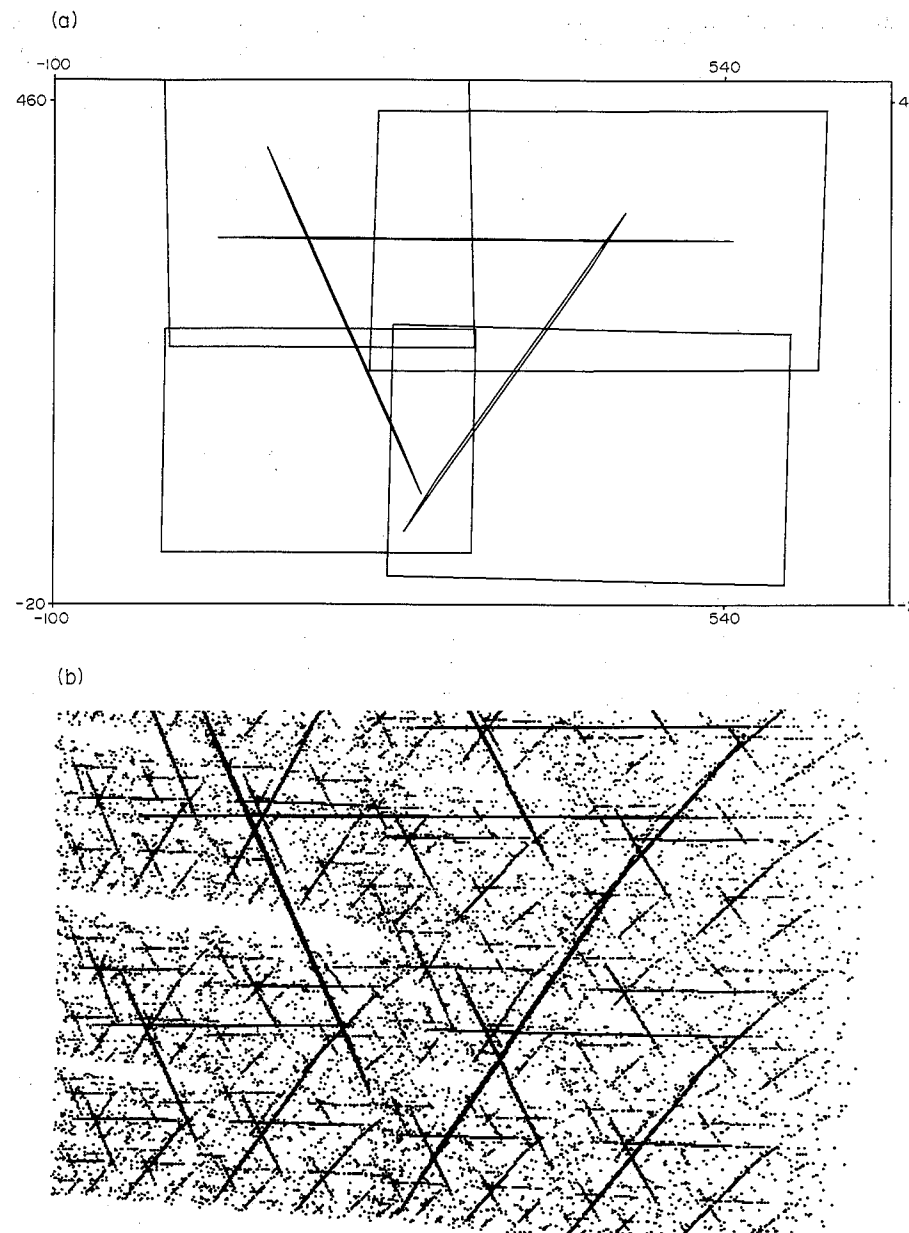


Figure 25 (a) Transformations representing the IFS which produces the joint system shown in (b)

Very realistic joint arrays are produced using these IFSs. This approach has considerable potential for reproducing and modeling the complicated joint arrays developed in nature. The important point to emphasize here is that the joint arrays presented here are produced in a purely deterministic manner. No scatter in spacing, orientation or persistence is introduced by applying random variation in the coefficients of the linear transformation employed. These transformations are intrinsically simple in structure although they map each transformation into each other in a random sequence. This procedure generates the irregular geometry portrayed in these diagrams without recourse to the addition of random variation to the coefficients themselves.

## 2.6 FOLD SYSTEMS

Application of the Collage Theorem (see Section 2.3.4) enables fold systems to be readily generated as fractal images. Figure 26 shows the transformations which result in a single layer fold

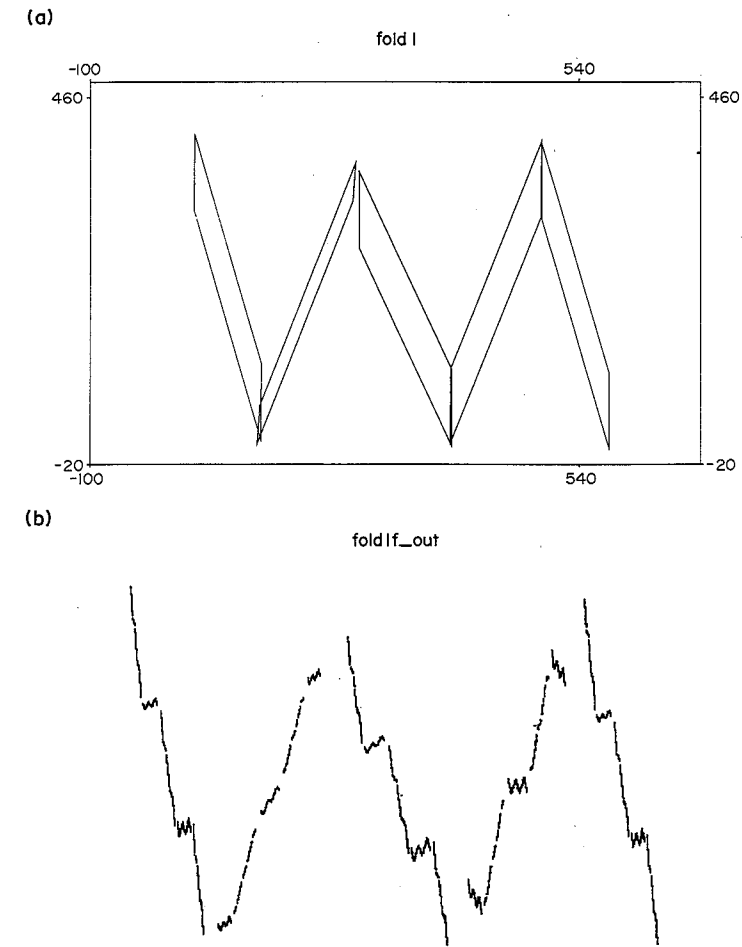


Figure 26 (a) Transformations representing the IFS which produces the single layer fold system shown in (b)

system. Notice that parasitic folds are an integral part of the system; this reflects a fine structure within the overall structure grossly defined by the transformations shown in Figure 26(a).

In Figure 27 a multilayer fold system has been generated with a crude axial plane structure developed.

## 2.7 CONCLUDING REMARKS

This chapter has been concerned with the structures that exist in rock masses which also influence the stability and mechanical behavior of those rock masses during and subsequent to excavation. The emphasis has been on two aspects of these structures, namely, the complexity and erratic nature of their geometry and the fact that these structures are duplicated at a number of scales; that is, the geometry is scale invariant.

These two qualities, complexity and scale invariance, are the two hallmarks of fractal geometry. Recognition of the fractal nature of structures in rock masses enables one to understand the ranges of spacings, orientations, thicknesses and persistences of structures observed in Nature. In particular, it has been shown that the geometric complexity observed in rock masses can be generated from simple deterministic rules involving the random mappings of space into itself using systems of affine transformations – iterated function systems (IFS) [59]. These iterated mappings also lead to scale invariance as the structures produced by each affine transformation are mapped back and forth into the other affine transformations.

Geometrical complexity arises in nonlinear systems when strong nonlinear feedback mechanisms are in operation between a number of processes [47]. In structural geology the dynamics of the

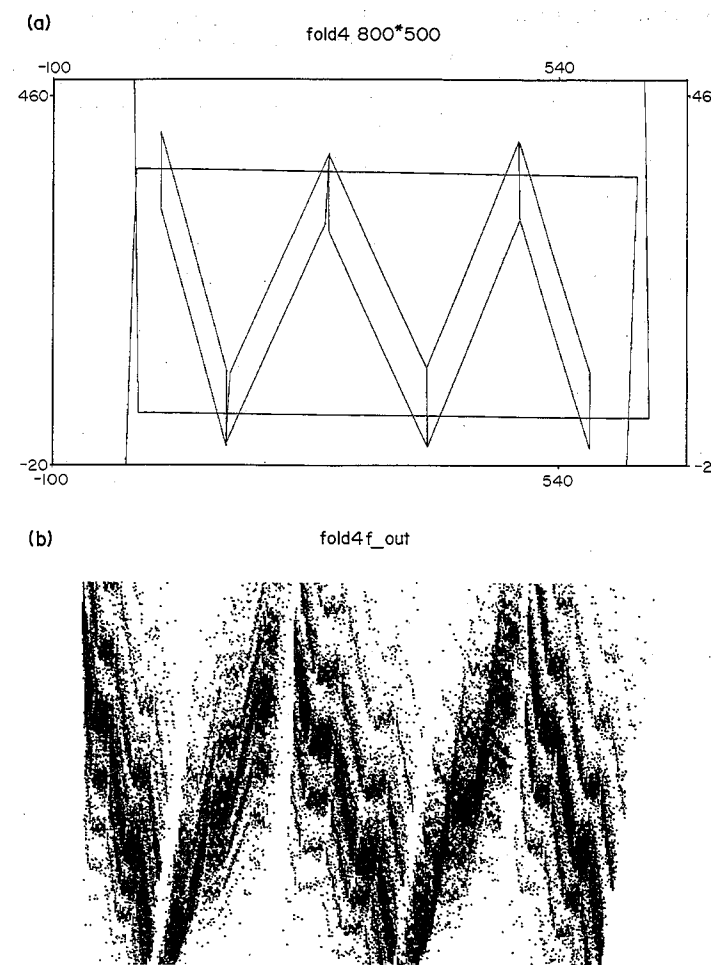


Figure 27 (a) Transformations representing the IFS which produces the multilayer fold system shown in (b)

deforming systems seem to be controlled by at least three nonlinear relations: the stress equations of motion, elastic-plastic deformation with the potential for local elastic unloading as prescribed by a yield criterion, and the noncoincidence of the plastic incremental strain vector with the normal to the yield surface, as prescribed by the flow rule [49].

These sets of equations lead to complexity in that initially homogeneously deforming systems can evolve into inhomogeneous deformation patterns which are not strictly periodic in their geometry [48, 49]. The nonlinear interactions between stress fields associated with each structure in the inhomogeneous deformation field enhances the complexity [48] and means that some structures can grow faster than others thus further enhancing the complexity. The interaction and feedback relations between adjacent structures [48] are similar in concept to the interactive mappings involved in the IFS generation of geometrical complexity and this prompts the suggestion that perhaps the IFSs are first order approximations to the nonlinear dynamical equations in state space that govern the development of structural complexity.

The overpowering questions in rock mechanics associated with structural geology are as follows.

(i) How does one represent the geometrical complexity observed in Nature so that this complexity can be taken into account in answering questions of stability and/or rock behavior?

(ii) Given that the geometry of structures is erratic with little apparent spatial order, how does one make predictions regarding the occurrence or nature of a particular type of structure within a particular volume of rock?

Needless to say, precise answers to these questions are still not available but appreciation of the fractal nature of structural geometry enables one to point towards the following answers.

(i) The Collage Theorem [59] sets the scene for representation of geometrical complexity. Several methods now exist [81, 82] for solving the inverse problem of specifying the IFS for an observed

geometry. This means that it is possible, in principle, to represent any observed distribution of joints, faults, or other structures by an IFS code. The geometrical complexity is thereby reduced to an array of coefficients which can be used at any future time to generate the geometry. This represents not only a concise way of describing structural complexity but is a way of achieving data compression for the storage of data. Since any complicated geometry can be generated by a relatively simple deterministic algorithm (the IFS), such an algorithm can be used as the basis of a fractal joint generator for use in computational procedures.

(ii) Since the geometry of structures in rock masses is deterministic and fractal, analogy with deterministic dynamical systems [47, 49, 83], suggests that the basic underlying deterministic geometry should be able to be represented for the observed geometry by constructing a spatial attractor [49] in phase space.

The principles involved here are demonstrated in Figure 28(a) where a periodic spatial distribution of joints is shown. In Figure 28(b) the results of laying a series of boxes across the joint array and

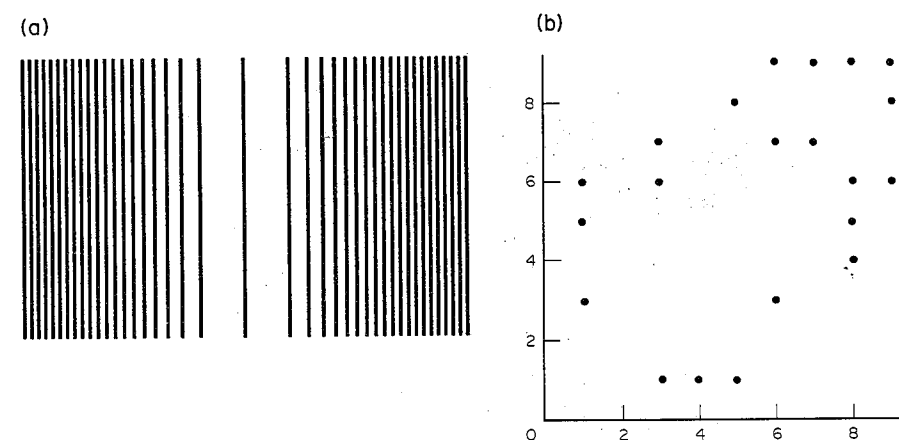


Figure 28 (a) Sinusoidal spatial distribution of joints. (b) Spatial attractor for geometry shown in (a).

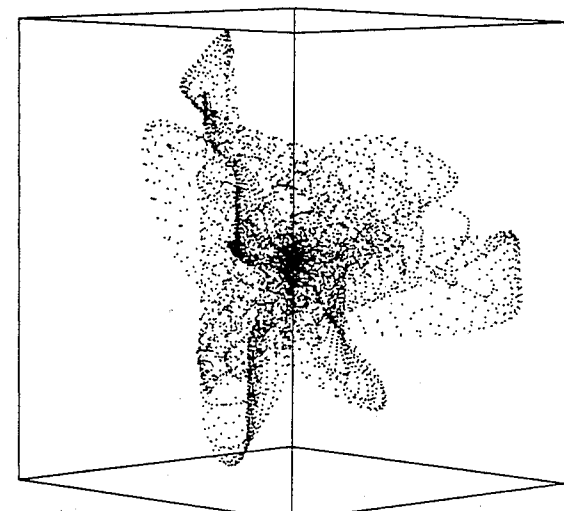


Figure 29 Spatial attractor derived from the velocity field of a numerically generated system of shear zones (after Ord [49])

plotting the number of joints in each box against the number of joints in a box two removed is presented. The result is an ordered distribution of points. Ord [49] has argued that constructions of this type are capable of reflecting the underlying nonlinear dynamics of the system.

Constructions such as those shown in Figure 28 and elaborated upon by Ord [49] are forms of generalized semivariograms [84] and are ways of representing the spatial correlations within a particular geometrical pattern. A complicated example of such a spatial attractor is shown in Figure 29. Ord shows that this attractor is fractal (but not chaotic) with a fractal dimension of 2.3 implying that three degrees of freedom were involved in the dynamics of the system which generated the underlying structure.

The important aspect of spatial attractors, as far as rock mechanics is concerned, is that they possess all the geometrical information necessary to discuss the spatial correlations between structures and thus form the basis for defining the probability whether a particular structure will exist at a specified point or not.

Although the study of fractal geometry with respect to structural geology is in its infancy, there is already a wealth of insight to be gained by examining the complexity and scale invariance of these structures from a fractal point of view. In particular, the realization that these structural geometries are deterministic and derive from well defined dynamical relations injects a level of understanding that has always been lacking and sets the scene for future well structured studies of the origins and forms of geometrical complexity in these structures [50].

## ACKNOWLEDGEMENTS

The work of Barnsley was introduced to me by Bob Perriam and I want to thank him for his foresight. This chapter is the result of many discussions with Frank Horowitz, Hans Mühlhaus, Alison Ord and Bill Power, and I thank them for their insight and inspiration.

## 2.8 REFERENCES

1. Turner F. J. and Weiss L. E. *Structural Analysis of Metamorphic Tectonites*, p. 545. McGraw-Hill, New York (1963).
2. Ramsay J. G. The deformation of early linear structures in areas of repeated folding. *J. Geol.* **68**, 75–93 (1960).
3. Ramsay J. G. *Folding and Fracturing of Rocks*, p. 568. McGraw-Hill, New York (1967).
4. Hobbs B. E., Means W. D. and Williams P. F. *An Outline of Structural Geology*, p. 571. Wiley, New York (1976).
5. Price N. J. and Cosgrove J. W. *Analysis of Geological Structures*, p. 502. Cambridge University Press, Cambridge (1990).
6. Barton N. and Choubey V. The shear strength of rock joints in theory and practice. *Rock Mech.* **8**, 1–54 (1977). Also Norwegian Geological Institute Publ. **119** (1978).
7. Wise D. U. Microjointing in basement, middle Rocky Mountains of Montana and Wyoming. *Geol. Soc. Am. Bull.* **75**, 287–306 (1964).
8. Scholtz C. H. Microfracturing and the inelastic deformation of rock in compression. *J. Geophys. Res.* **73**, 1417–1732 (1968).
9. Parker J. M. Regional systematic jointing in slightly deformed sedimentary rocks. *Geol. Soc. Am. Bull.* **53**, 381–408 (1942).
10. Hodgson R. A. Classification of structures on joint surfaces. *Am. J. Sci.* **259**, 493–502 (1961).
11. Roberts J. C. Feather-fracture and the mechanics of rock-jointing. *Am. J. Sci.* **259**, 481–492 (1961).
12. Von Bankwitz P. Über Klufte I, beobachtungen in thüringischen schierengebirge. *Geolog. Z. Gesamtgebiet Geologie Mineralogie* **14(H3)**, 241–253 (1965). Von Bankwitz P. Über Klufte, II. *Geologie* **15**, 896–941 (1966).
13. Price N. J. *Fault and Joint Development in Brittle and Semi-Brittle Rock*, p. 176. Pergamon Press, New York (1966).
14. Syme-Gash P. J. A study of surface features relating to brittle and semi-brittle fracture. *Tectonophysics* **12**, 349–391 (1971).
15. McClintock F. A. and Argon A. S. *Mechanical Behaviour of Materials*, p. 770. Addison-Wesley, Reading, MA (1966).
16. Park C. F. and MacDiarmid R. A. *Ore Deposits*, p. 522. Freeman, San Francisco (1964).
17. Norris D. K. Structural analysis of the Queensway folds, Ottawa, Canada. *Can. J. Earth Sci.* **4**, 299–321 (1967).
18. Stearns D. W. Certain aspects of fractures in naturally deformed rocks. In *NSF Advanced Science Seminar in Rock Mechanics for College Teachers of Structural Geology* (Edited by R. E. Riecher), Terrestrial Science Laboratory Air Force, Cambridge Research Laboratories, MA (1968).
19. Handin J., Friedman M., Logan J. M., Pattison L. J. and Swolfs H. S. Experimental folding of rocks under confining pressure: buckling of single-layer rock beams. In *Flow and Fracture of Rocks* (Edited by H. C. Heard, I. Y. Borg, N. L. Carter and C. B. Raleigh), *Geophys. Monogr. Am. Geophys. Union* **16** (1972).
20. Cloos E. 'Feather joints' as indicators of the direction of movements on faults, thrusts, joints and magmatic contacts. *Geology* **18**, 387–395 (1932).
21. Morgenstern N. R. and Tchalenko J. S. Microscopic structures in kaolin subjected to direct shear. *Géotechnique* **17**, 309–328 (1967).
22. Lajtai E. Z. Mechanics of second order faults and tension gashes. *Geol. Soc. Am. Bull.* **80**, 2253–2272 (1969).
23. Gay N. C. The formation of step structures on slicksided shear surfaces. *J. Geol.* **78**, 423–532 (1970).

24. Friedman M. and Logan J. M. Microscopic feather fractures. *Geol. Soc. Am. Bull.* **81**, 3417–3420 (1970).
25. Dunn D. E., LaFountain L. J. and Jackson R. E. Porosity dependence and mechanism of brittle fracture in sandstones. *J. Geophys. Res.* **78**, 2403–2417 (1973).
26. Balk R. Structural behaviour of igneous rocks. *Mem. Geol. Soc. Am.* **5** (1937).
27. Spry A. The origin of columnar jointing, particularly in basalt flows. *J. Geol. Soc. Aust.* **8**, 191–216 (1962).
28. Twiss R. J., Protzman G. M. and Hurst S. D. Theory of slickline patterns based on the velocity gradient tensor and microrotation. *Tectonophysics* **186**, 215–239 (1991).
29. Griggs D. and Handin J. Observations on fracture and a hypothesis of earthquakes. In *Rock Deformation* (Edited by D. Griggs and J. Handin) *Proc. Vol. Geol. Soc. Am.* **79**, 347–373 (1960).
30. Jahns R. H. Sheet structure in granites: its origin and use as a measure of glacial erosion in New England. *J. Geol.* **LI(2)**, 71–98 (1943).
31. Johnson A. M. *Physical Processes in Geology*, p. 577. Freeman, San Francisco (1970).
32. Birch F. Compressibility; elastic constants. In *Handbook of Physical Constants* (Edited by S. P. Clark), *Mem. Geol. Soc. Am.* **97**, 97 (1966).
33. Iddings J. P. Columnar structure in the igneous rocks of Orange Mtn., N.J. *Am. J. Sci.* **131**, 321–330 (1886).
34. James A. V. G. Factors producing columnar structure in lavas and its occurrence near Melbourne, Australia. *J. Geol.* **28**, 458–471 (1920).
35. McKenzie D. P. Plate tectonics. In *The Nature of the Solid Earth* (Edited by E. C. Robertson), pp. 323–360. McGraw-Hill, New York (1972).
36. Turcotte D. L. and Oxburgh E. R. Mid-plate tectonics. *Nature (London)* **244**, 337–339 (1973).
37. Dennis J. G. *International Tectonic Dictionary*, p. 196. American Association of Petroleum Geologists, Tulsa, OK (1967).
38. Hills E. S. *Elements of Structural Geology*, 2nd edn., p. 502. Wiley, New York (1972).
39. Billings M. P. *Structural Geology*, p. 606. Prentice Hall, Englewood Cliffs, NJ (1972).
40. Potter P. E. and Pettijohn F. J. *Paleocurrents and Basis Analysis*, p. 296. Springer-Verlag, Berlin (1963).
41. Vernon R. H. The Willyama complex, Broken Hill area. In *The Geology of NSW* (Edited by G. H. Packham). *J. Geol. Soc. Aust.* **16**, 20–55 (1969).
42. Hudson J. A. and Priest S. D. Discontinuities and rock mass geometry. *Int. J. Rock Mech. Min. Sci. & Geomech. Abstr.* **16**, 339–362 (1979).
43. Hudson J. A. and La Pointe P. R. Printed circuits for studying rock mass permeability. *Int. J. Rock Mech. Min. Sci. & Geomech. Abstr.* **17**, 297–301 (1980).
44. La Pointe P. R. and Ganow H. C. Successful prediction of in situ fracture permeability and stiffness characteristics through statistical rock mass characterization. In *Proc. 25th U.S. Symp. Rock Mech.*, Evanston, IL, pp. 409–416. SME/AIME, New York (1984).
45. La Pointe P. R. and Hudson J. A. Characterization and interpretation of rock mass joint patterns. *Spec. Pap. Geol. Soc. Am.* **199** (1985).
46. Barton C. A. and Zoback M. D. Self-similar distribution of macroscopic fractures at depth in crystalline rock in the Cajon Pass scientific drill hole. In *Rock Joints* (Edited by N. Barton and O. Stephansson), pp. 163–170. Balkema, Rotterdam (1990).
47. Prigogine I. and Stengers I. *Order Out of Chaos*, p. 349. Bantam, New York (1984).
48. Cundall, P. Shear band initiation and evolution in frictional materials. In *Proc. ASCE Eng. Mech. Speciality Conference*, Columbus, OH (1991).
49. Ord A. The geometry of patterned structures. *J. Struct. Geol.* In press (1993).
50. Mühlhaus H. B. Evolution of elastic folds in plane strain. In *Modern Approaches to Plasticity* (Edited by D. Kolymbas), Springer-Verlag, Berlin. In press (1993).
51. Biot M. A. *Mechanics of Incremental Deformation*, p. 504. Wiley, New York (1965).
52. Ramberg H. Fluid dynamics of viscous buckling applicable to folding of layered rocks. *Am. Assoc. Pet. Geol. Bull.* **47**, 485–505 (1963).
53. Feder J. *Fractals*, p. 283. Plenum Press, New York (1988).
54. Mandelbrot B. B. *The Fractal Geometry of Nature*, p. 468. Freeman, San Francisco (1982).
55. Power W. L. and Tullis T. E. A review of the fractal character of natural fault surfaces with implications for friction and the evolution of fault zones. In *Fractals and their Application to Geology* (Edited by C. C. Barton and P. R. La Pointe), Geological Society of America, Boulder, CO. In press (1993).
56. Barton C. C. and Larsen E. Fractal geometry of two-dimensional fracture networks at Yucca Mountain, Southwestern Nevada. In *Proc. Int. Symp. Fundamentals of Rock Joints*, Bjorkliden, Sweden (Edited by O. Stephansson), pp. 77–84. Centek, Luleå, Sweden (1985).
57. Pruess S. Some remarks on the numerical estimation of fractal dimension. In *Fractals and their Application to Geology* (Edited by C. C. Barton and P. R. La Pointe), Geological Society of America, Boulder, CO. In press (1993).
58. Barnsley M. F. and Demko S. Iterated function systems and the global construction of fractals. *Proc. R. Soc. London, Ser. A* **399**, 243–275 (1985).
59. Barnsley M. F. *Fractals Everywhere*, p. 396. Academic Press, New York (1988).
60. Jügens H., Peitgen H.-O. and Saupe D. The language of fractals. *Sci. Am. August*, 60–67 (1990).
61. Brown S. R. A note on the description of surface roughness using fractal dimension. *Geophys. Res. Lett.* **14**, 1095–1098 (1987).
62. Wong P. Fractal surfaces in porous media. In *Physics and Chemistry of Porous Media II, AIP Conf. Proc.* **154** (Edited by J. Banavar, J. Koplik and K. Winkler), pp. 304–318. American Institute of Physics, New York (1987).
63. Brown S. R. and Scholz C. H. Broad bandwidth study of the topography of natural rock surfaces. *JGR, J. Geophys. Res.* **90**, 12 575–12 582 (1985).
64. Lee Y.-H., Carr J. R., Barr D. J. and Hass C. J. The fractal dimension as a measure of the roughness of rock discontinuity profiles. *Int. J. Rock Mech. Min. Sci. & Geomech. Abstr.* **27**, 453–464 (1990).
65. Barton N. A relationship between joint roughness and joint shear strength. In *Proc. Int. Symp. Rock Fracture*, Nancy, France, paper I.8 (1971).
66. Barton N. and Choubey V. The shear strength of rock joints in theory and practice. *Rock Mech.* **8**, 1–54 (1977). Also NGI-Publ. **119** (1978).

67. Barton N. and Bandis S. Review of predictive capabilities of JRC-JCS model in engineering practice. In *Proc. Int. Conf. Rock Joints*, Loen, Norway (Edited by N. Barton and O. Stephansson), Balkema, Rotterdam (1990).
68. Turk N., Greig M. J., Dearman W. R. and Amin F. F. Characterization of rock joint surface by fractal dimension. In *Proc. 28th U.S. Symp. Rock Mech.*, Tucson, AZ (Edited by I. W. Farmer, J. J. K. Daemen, C. S. Desai, C. E. Glass and S. P. Neuman), pp. 1223–1236. Balkema, Rotterdam (1987).
69. Carr J. R. and Warriner J. B. Rock mass classification using fractal dimension. In *Proc. 28th U.S. Symp. Rock Mech.*, Tucson, AZ (Edited by I. W. Farmer, J. J. K. Daemen, C. S. Desai, C. E. Glass and S. P. Neuman), pp. 73–80. Balkema, Rotterdam (1987).
70. Carr J. R. Relationship between the fractal dimension and joint roughness coefficient. *Bull. Assoc. Eng. Geol.* **26**, 253–263 (1989).
71. Carr J. R. Fractal characterization of joint surface roughness in welded tuff at Yucca Mountain, Nevada. In *Proc. 30th U.S. Symp. Rock Mech.* (Edited by A. W. Khair), pp. 193–200 (1989).
72. Carr J. R. Stochastic versus deterministic fractals; the controversy over applications in the earth sciences. In *Engineering Geology and Geotechnical Engineering* (Edited by R. J. Watters), pp. 297–308. Balkema, Rotterdam (1989).
73. Maerz N. H., Franklin J. A. and Bennett C. P. Joint roughness measurement using shadow profilometry. *Int. J. Rock Mech. Min. Sci. & Geomech. Abstr.* **27**, 329–343 (1990).
74. Power W. L. and Tullis T. E. Euclidean and fractal models for the description of rock surface roughness. *J. Geophys. Res.* **96**, 415–424 (1991).
75. Miller S. M., McWilliams P. C. and Kerkering J. C. Ambiguities in estimating fractal dimensions of rock fracture surfaces. In *Proc. 31st U.S. Symp. Rock Mech.*, Golden, CO (Edited by W. Hustrulid and G. A. Johnson), pp. 471–478. Balkema, Rotterdam (1990).
76. Priest S. D. and Hudson J. A. Discontinuity spacings in rock. *Int. J. Rock Mech. Min. Sci. & Geomech. Abstr.* **16**, 339–363 (1976).
77. Einstein H. H. and Baecher G. B. Probabilistic and statistical methods in engineering geology. *Rock Mech. Rock Eng.* **16**, 39–72 (1983).
78. Rouleau A. and Gale J. E. Statistical characterization of the fracture system in the Stripa Granite, Sweden. *Int. J. Rock Mech. Min. Sci. & Geomech. Abstr.* **22**, 353–367 (1985).
79. Bardsley W. E., Major T. J. and Selby M. J. Note on a Weibull property for joint spacing analysis. *Int. J. Rock Mech. Min. Sci. & Geomech. Abstr.* **27**, 133–134 (1990).
80. Velde B., Dubois J., Touchard G. and Badri A. Fractal analysis of fractures in rocks: the Cantor's Dust methods. *Tectonophysics* **179**, 345–352 (1990).
81. Jacquin A. E. Image coding based on a fractal theory of iterated contractive image transformations. *IEEE Trans. Sig. Proc.* (1992). Also in Course 14 Notes, ACM SIGGraph (1991).
82. Vrscay E. R. Moment and collage methods for the inverse problem of fractal construction with iterated function systems, In *Fractals in the Fundamental and Applied Sciences* (Edited by H.-O. Peitgen, J. M. Henquieres and L. F. Penedo), pp. 443–461. Elsevier, New York (1991).
83. Packard N. H., Crutchfield J. P., Farmer J. D. and Shaw R. S. Geometry from a time series. *Phys. Rev. Lett.* **45**, 712–716 (1980).
84. Villaescusa E. and Brown E. T. Characterizing joint spatial correlation using geostatistical methods. In *Rock Joints* (Edited by N. Barton and O. Stephansson), pp. 115–122. Balkema, Rotterdam (1990).

## Natural Rock

### University of Manchester, UK

3.1 INTRODUCTION	63
3.2 THE PHILOSOPHY AND EXPERIMENTAL TECHNIQUES OF GEOLOGICALLY ORIENTED ROCK MECHANICS	64
3.3 MECHANISMS OF ROCK DEFORMATION AND MODES OF FAILURE	67
3.4 A CLOSER LOOK AT THE DIFFERENT DEFORMATION MECHANISMS	68
3.4.1 Cataclastic Deformation	68
3.4.2 Intracrystalline Plasticity	72
3.4.2.1 Constitutive flow laws	76
3.4.2.2 Role of intergranular fluids in plastic flow	77
3.4.2.3 Preferred crystallographic orientation	77
3.4.2.4 Mechanical twinning	78
3.4.3 The Brittle-Ductile Transition	79
3.4.4 Flow by Diffusive Mass Transfer	82
3.4.5 Deformation Mechanism Maps	84
3.4.6 High Temperature Flow of Fine-grained Rocks	85
3.4.7 Rock Deformation and Metamorphism	87
3.5 RHEOLOGICAL STRATIFICATION OF THE LITHOSPHERE	88
3.6 ECONOMIC IMPLICATIONS OF NATURAL ROCK DEFORMATION	90
3.7 SUMMARY AND CONCLUSIONS	90
3.8 REFERENCES	91

### 3.1 INTRODUCTION

Whereas the engineer is concerned principally with rock deformation and failure under conditions of loads caused by or modified through excavations, buildings or natural topography, rocks are commonly found which have been deformed by natural tectonic forces. The range of natural rock structures and microstructures is extremely wide, reflecting deformation over a wide range of confining and pore fluid pressures, strain rates, temperatures and shear strains.

The deformed state of a rock may be important to the engineer for several reasons. Anisotropy of mechanical and other properties may have developed, which can affect the way the material must be worked. Residual stresses may be stored, capable of affecting *in situ* stress determinations or of causing time-dependent failure of the material even when not loaded by external forces. Faults may be present in the rock mass and, depending on the nature of the engineering activity, may have to be regarded as potential zones of fluid channeling, or of reactivation, even in intraplate situations.

Structural and microstructural studies (structural petrology) of the *in situ* rocks or of samples retrieved from boreholes represent an important way that we can learn about natural rock deformation. Additional information from mechanical tests on rocks, conducted over a range of